Travail de fin d'études et stage[BR]- Travail de fin d'études : Experimental characterization of an air-water propane heat pump and case study[BR]- Stage d'insertion professionnelle

Auteur : Daems, Olivier
Promoteur(s) : Lemort, Vincent
Faculté : Faculté des Sciences appliquées
Diplôme : Master en ingénieur civil électromécanicien, à finalité spécialisée en énergétique
Année académique : 2021-2022
URI/URL : http://hdl.handle.net/2268.2/15562

Liege University
Faculty of Applied Sciences
Electromechanical department

Master's thesis presented and defended by:
Daems Olivier

Experimental characterization of an air-water propane heat pump and case study

Jury:

Renhman Danish, Mitis
Lemort Vincent, Uliege
Dumont Olivier, Uliege
Gendebien Samuel, Uliege

Promotor: Lemort Vincent
Supervisor: Renhman Danish

Academic year 2021-2022

Acknowledgements

I would like to take this opportunity to express my sincere thanks to all those who helped me, accompanied me, and supported me during the period of my master's thesis.

Special thanks go to my company supervisor, Danish Renhman, without whom I could not have achieved this work. His valuable help and advice were very important during the intership.

I also would like to thank all the member of the Thermodynamics Laboratory of Liege. Thanks to Richard Labenda for helping me during the implementation of the test bench; to Mazarine Roquet for her explanation regarding the modeling program Dymola.

I would like to thank Professor Vincent Lemort for guiding me during the realization of this thesis.

I am grateful to Hugo Luca who shared his results as part of a joint project, which allowed me to have a study based on a real case.

Finally, I would like to express my greatest gratitude to my parents for their motivation and encouragements. Thanks a lot also to Jean-Louis Van Den Haute for his correction of the writing.

Abstract

This master thesis presents an experimental analysis of a 10 kW air-to-water propane heat pump, as part of the Flaminco research project that has been carried out by *Mitis*. With regard to legislation concerning heating and air conditioning, propane is a natural gas that could be a substitute refrigerant for polluting refrigerants. The work involes four mains parts: preparation of the HP unit test rigs, experimental campaign, the evaluation of test results and a case study with a load profil.

The experimental compaign is mainly focused on the performance in the heating mode of the heat pump, and is also studied in cooling mode. The performance of the compressor and the system is studied with different operating points and against external parameters such as air temperature and water temperature.

The case study was made with Dymola using preimplemented libraries. The heating system is composed of a gas turbine, a storage tank, a condensing boiler and a known load. The load profile is given and the models are adapted to match the real machines. The interest is to see the impact of the regulation system on the economic aspect for one year.

Contents

List of Figures

List of Tables

Nomenclature

Acronym

AC Alternative current

$BPHE$ Brazed plate heat exchanger

CHP Combined heat and power

COP Coeffcient Of Performance

DC Direct current

EER Energy efficiency ratio

EEV Electronic expansion valve

GHG Greenhouse gases

GWP Global warming potential

HP Heat pump

ODP Ozone depletion potential

$PFHE$ Plate-fin heat exchanger

RES Rewable energy sources

RPM Rotation per minute

TMY Typical Meteorological Year

Exponents and subscripts

air Outside air

$calculated$ Calculated

$Carnot$ Relating to the carnot cycle

cd Condenser

cp Compressor

dis Discharge line

eev Electronic expansion valve

el Electrical

ev Evaporator

$fans$ Fans

fhe Fin heat exchanger

fl Full load

gas Gas

HO Heating oil

II Second-law

in Inlet

is Isentropic

n, nom Nominal

on, off Activation, deasctivation

out Oulet

p Constant pressure

phe Plate heat exchanger

pl Partial load

r Refrigerant

s Swept

$sell$ Selling

suc Suction line

sup Additional heat

th Theoritical

tot Total

vol Volumetric

w Water

Symbols

$\dot{m}$ Mass flow rate

$\dot{Q}$ Thermal power

$\dot{V}$ Volumetric flow rate

$\dot{W}$ Power

ϵ Efficiency

η Yield

π Market price

ρ volumic mass

C Thermal capacity

C Cost

c Specific heat capacity

G Thermal conductance

h Enthalpy

N Rotational speed

P	Pressure
s	Entropy
T	Temperature
U	Boolean variable
V	Volume

Chapter 1

Introduction

1.1 Climatic and political context

Since the industrial revolution of the early 19th century, many climate changes have been observed: ozone holes, melting ice, climate deregulation, temperature rises, etc. They are the consequences of the intensive emission of greenhouse gases (GHGs) and the overconsumption made by humans. These disasters have caused the extinction of numerous plants and animals and really threaten human lives.

During the last years, controls and objectives are imposed in many sectors to restore global balance. The Paris agreement that includes 193 parts aims to limit global warming to 2 ° C by 2100 compared to pre-industrial levels. The average temperature has already increased by 1.2 ° C [1]. The ultimate goal is to achieve total decarbonization for an acceptable standard of living.

Regarding the European Union, the objective in 2008 was to reduce the emission of GHG and the energy consumption by 20% and increase the renewable energy sources (RES) in the portfolio by 20% as well. An update was implemented in 2014 to raise the levels to 40%, 27% and 27%, respectively, for 2030 [2]. Decreasing the consumption could be the most simple part because it will automatically solve the other problems, but it required both the effort of humans in everyday life and the imporvement of energetic efficiency. Therefore, there is a growing interest in the research of alternative solutions or high efficiency processes to live confortably by poluting as little as possible.

One of the main sectors in terms of energy consumption is residential. According to SPF economie [3], in 2020 in Belgium, 7,9 Mtoe has been required, equivalent to 20,8% of total consumption. The use of energy for this sector goes mainly to the heating of

buildings with 73,2%. Therefore, energy management in buildings is a crucial element in the race to achieve the carbon neutrality objective. From one hand, it is important to improve the buildings structure such as insulation, location,... and from the other, to improve the heating systems providing the energy. Heat pumps, which work with refrigerants, could then represent an alternative thank to their low carbon emission.

Refrigerants are classified according to their global warming potential (GWP) over 100 years and their ozone depletion potential (ODP) and there is a very serious legislation concerning them. The reference for the GWP is CO2 and R11 for the ODP, one of the most harmful fluids. There are four types of refrigerants: CFC, HCFC, HFC and PFC [1]. Systems working with those fluids are never 100% tight and can slowly reject gases to the atmosphere. Also, when the machine is at its end of life, fluids cannot always be recycled.

CFCs, which have the most dangerous ODP (close to one, therefore identical to R11) and GWP (4660 to 13900 [4]), have not been produced anymore since 1995 [5] as a result of the Montreal protocol in 1987 targeting substances that deplete the ozone layer. R11 which was the first commonly used refrigerant is a CFC.

After that, HCFCs production is more and more reduced due to their high GWP (1 to 12400 [4]) and ODP (0 to 1 [6]) until their total ban in 2015. R22 is an example of HCFC (see Table 1.2).

The next step is to abolish HFC in 2030 so that only the refrigerant with the lowest GWP and ODP could be used. For a refrigerant to be allowed on refrigeration installations in 2030, it must have a GWP of less than 150 [7].

Another classification is based on the level of toxicity and inflammability. The following table 1.1 provides an overview of the ASHRAE Standard 34 (2019) refrigerant safety group classification.

	lower toxicity	higher toxicity
higher flammability	A3	B3
lower flammability	A2	B2
	A2L	B2L
no flame propagation	A1	B1

Table 1.1: Refrigerant classification from ASHRAE Standard 34 [8]

Another practical criterion is, of course, the performance in the field of application.

[1] CFC: chlorofluorocarbure, HCFC: hydrochlorofluorocarbure, HFC: hydrofluorocarbure, PFC: Perfluorocarbure

Choosing a low-GWP and ODP refrigerant is necessary, but it should also provide good efficiency, depending on the application. The saturation curve is then an important feature to look at, especially at evaporating and condensing temperatures. Also, the higher the amount of energy absorbed, the better.

Alternative refrigerants for the future are detailed in the following section.

1.2 Heating systems review

Heating a house is probably the largest energy expense; 35% to 50 % of the annual energy bills according to *SmarterHouse* [9]. It is also a huge source of CO2 emission. There are many types of heating systems in buildings that can be centralized or direct. Central heating usually provides heat or hot water for the whole building, while direct heating is used only when and where needed. Depending on the case, one is more efficient. For example, schools or apartment buildings that need full heating may require a centralized system rather than direct heating.Among the most common centralized systems are furnaces, boilers, heat pumps, ... and even combined heat and power.

Furnaces and boiler

Furnaces work by injecting a flow of hot air with fans directly into the house. Air is heated via a heat exchanger connected to the combustion chamber where oil or gas are burned. The downside is that combustion products are rejected to the atmosphere, wasting some of the heat and polluting . Boilers use the same process, but water is used as a working fluid and requires radiators and hydraulic pumps. Figure 1.1 shows a boiler equipped with a tank to provide hot water and a furnace to produce hot air. Nowadays, boilers use condensing technology to make better use of the heat they generate from burning fuels. One of the products in the combustion chamber is water steam. A condensing boiler extracts additional heat by condensing this water steam to liquid water, thus recovering its latent heat of vaporization. Condensing boiler manufacturers claim that up to 98% of thermal efficiency can be achieved [10] compared to 60-40 % for conventional boilers.

Heat pump

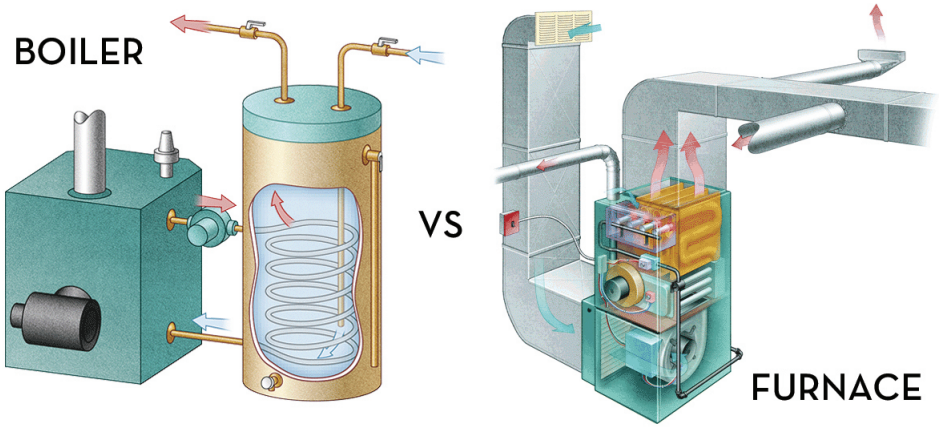

Figure 1.1: Diagram of a boiler (left) and furnace (right). Source: [11]

Heat pumps (HP) are machines that transfer heat from a lower temperature source to an higher temperature sink by consuming electricity. It could provide heating, cooling (reverse cycle), or hot water for residential, commercial, and industrial applications. The device could also provide both heating and cooling in parallel.

This mechanism is carried out through a refrigerant cycle composed of a compressor, a condenser, an expansion valve, and an evaporator. When a working fluid changes state, latent heat is exchanged and can be used. The cycle is represented in Figure 1.2 as a heating system with its main components. An heat pump in heating mode automatically produces cold as well but what matters is useful work. In this case, the purpose is to extract energy from the source, which could be outside air, a geothermal circuit, a lake, etc., and to reject it to a sink providing a heating system. Heat pumps are commonly classified by the source and sink type: a water-to-air heat pump sucking heat from a water source to an air sink. The ideal cycle is generally studied through 4 main steps of the refrigerant:

- 1-2: Isentropic compression of the refrigerant in gaseous state by consuming electrical work $\dot{W}_{cp}$. The compressor could be a scroll, piston, screw, etc.
- 2-3: Isobaric condensation of the refrigerant in an heat exchanger to provide useful heat $\dot{Q}_{cd}$ at higher temperature to house. Heat can be transfer to water for sanitary, radiator or floor heating, or to air for conditioning system.
- 3-4: Isenthalpic expansion of the liquid refrigerant to reduce pressure.

- 4-1: Isobaric evaporation of the refrigerant in a heat exchanger absorbing $\dot{Q}_{ev}$ at lower temperature. Heat can be sucked from air, water through an open loop (sea, lake, etc.) or from the ground through a closed loop.

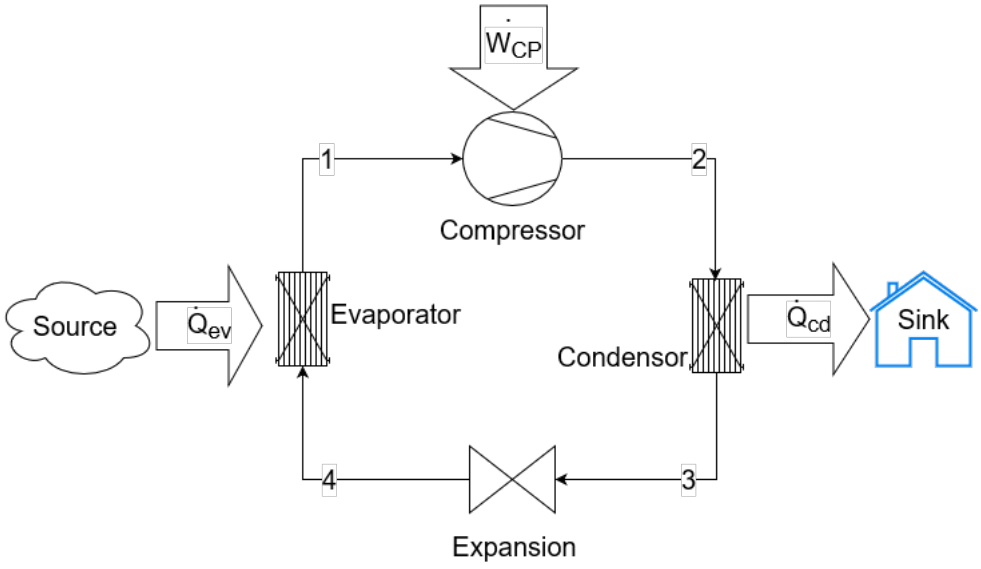

Figure 1.2: Heat pump circuit

In a real cycle, there are pressure losses, ambient heat losses, and no isentropic compression. In addition, two steps must be added compared to the ideal cycle. The compressor should always work with gaseous state for security and efficiency reasons. An overheating (4'-1) is then required in the evaporator. Subcooling (2'-3) in the condenser is also important to ensure proper operation of the expansion valve. Figure 1.3 shows the evolution of the refrigerant states of a real heat pump cycle on a temperature / entropy (Ts) diagram. The red color represents the refrigerant circuit while the color dark is its saturation curve.

As stated befor, choosing the refrigerant is crutial for heat pump performance and application. It should also match the legislation regarding GWP, ODP, toxicity, and inflammability.

Natural fluids such as water, CO2, ammonia, etc. could be used as a refrigerant in heat pumps.

Water or R718 has no GWP and ODP, is not flammable, no toxic, in short, the perfect refrigerant. It has shown good efficiency, especially in high-temperature heat

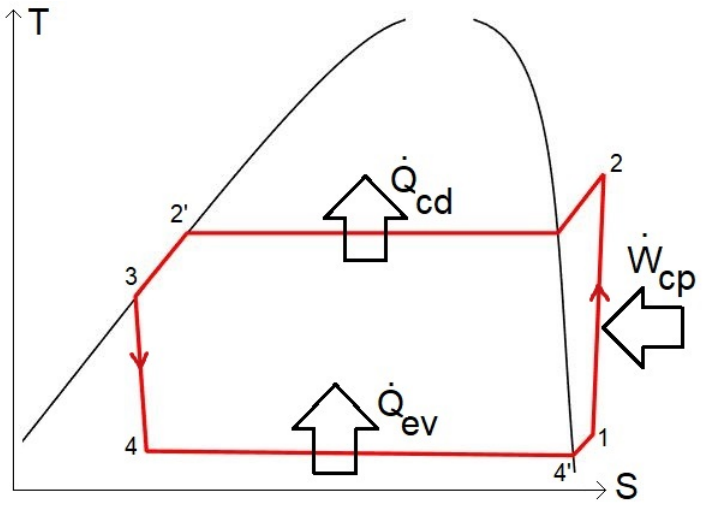

Figure 1.3: T-S diagram of a heat pump cycle

pumps [12]. However, it presents two significant disadvantages: it freezes below 0 ° C and has a high boiling temperature. Low pressure must then be reached (5-200 mbar [13]).

With its GWP = 1 and zero ODP [4], CO2 or R744 is also a studied gas for heat pumps. Its is inflammable, no toxic and cheap. Because of its very low critical temperature, a transcritical operation is required and then pressure ratio has to be very high to reach good running condition. This implies the use of more robust pipes and components for security reasons, and then increases the cost of installation.

Ammonia or R717 is another toxic and flammable natural refrigerant, and it can absorb and release more heat through one cycle [14]. It has a 0-GWP and 0-ODP but could be very dangerous in case of leak because of its toxicity. Additionally, ammonia can react with the copper of the pipes.

Some of the hydrocarbons (HCs) are also natural refrigerants. Propane (R290), butane (R600a) and isobutane (R600) are the main promising HCs and have less GWP (<150) and zero ODP [4] and are known for their very good thermodynamic properties in heat pumps [15] [16]. They are not toxic but extremely flammable (A3) and require very safe conditions. Propane is generally known as a domestic and industrial fuel, but it is increasingly being studied and used as a refrigerant for a refrigeration machine. As shown in Figure 1.4, the number of articles dealing with propane in heat pumps has increased over the past decade. It has been studied for many applications of refrigeration machines, such as electric vehicles [17] and freezers [18], for example.

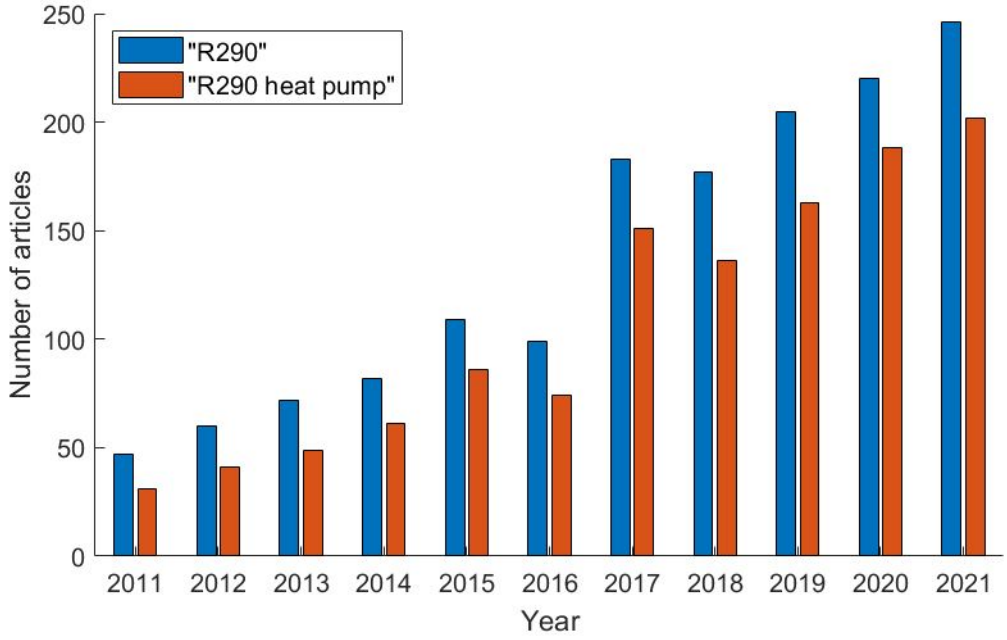

Figure 1.4: Evolution of the number of articles published on Science Direct

The interest in R290 is great due to its performance in refrigeration machine compared to common HCFs such as R404A and R134a [19] [20]. It allows the use of a reduced mass charge, low generation temperature, and no metal corrosion [21].

Some of the Hydrofluoroolefins (HFOs) have also low GWP and zero ODP [4]. R1234yf is found to be a promising substitute for replacing current high-GWP HFCs fluids. It has 100-year GWP <1 [22][23] but has lower performance than R290 [24]. One can use R1234yf instead of R290, where flammability is a concern.

For all its positive aspects and future prospects, R290 is the working fluid of the heat pump studied in this thesis.

Table 1.2 resumes all refrigerants that have been mentioned.

Micro combined heat and power

Combined heat and power (CHP) or cogeneration is a technology that produces both electricity and heat through one process to use of more of the chimical energy in the fuel. The yield in traditional power plants is approximately 30-40 % of the primary energy [26], such as coal, natural gas, uranium, petrol, etc. In contrast, CHP can convert 15 to 42% of fuel energy into heat while most of remaining heat is captured

Type	ASHRAE number	Chemical name	100-years GWP	ODP	Standard 34 [25]
CFC	R11	Trichloro-fluoromethane	4,660	1	A1
HCFC	R22	Chloro-difluoromethane	1,760	0.055	A1
Natural refrigerant	R718	Water	0.2	0	A1
Natural refrigerant	R744	Carbon dioxide	1	0	A1
Natural refrigerant	R717	Ammonia	0	0	B2L
HC	R290	Propane	3	0	A3
HC	R600a	Butane	5	0	A3
HC	R600	Isobutane	3	0	A3
HCF	R404a	Mixture R-125/143a/134a	3,9	0	A1
HCF	R134a	1,1,1,2-Tetra-fluoroethane	1300	0	A1
HFO	R1234yf	2,3,3,3-Tetra-fluoropropene	1	0	A2L

Table 1.2: Summary of main refrigerants

making a total of 90 % of energy yield.

Different types of power plants include the piston engine, the steam turbine, the gas turbine, some fuel cells, nuclear, and even renewable energy.

Figure 1.5 shows the principle of a common CHP based on a gas turbine [27]. A gaseous fluid is compressed before entering a combustion chamber where the primary energy is consumed. The fuel used is typically natural gas. Hot gas is relaxed in a turbine to produce electricity with a generator connected to the grid and the building. Heat remains in the exhaust gas (at 80-150 °C) and can be recovered through a heat exchanger to supply the building. Heat cannot be transported or stored, so it has to be consumed directly. Gas turbine are very flexible machine.

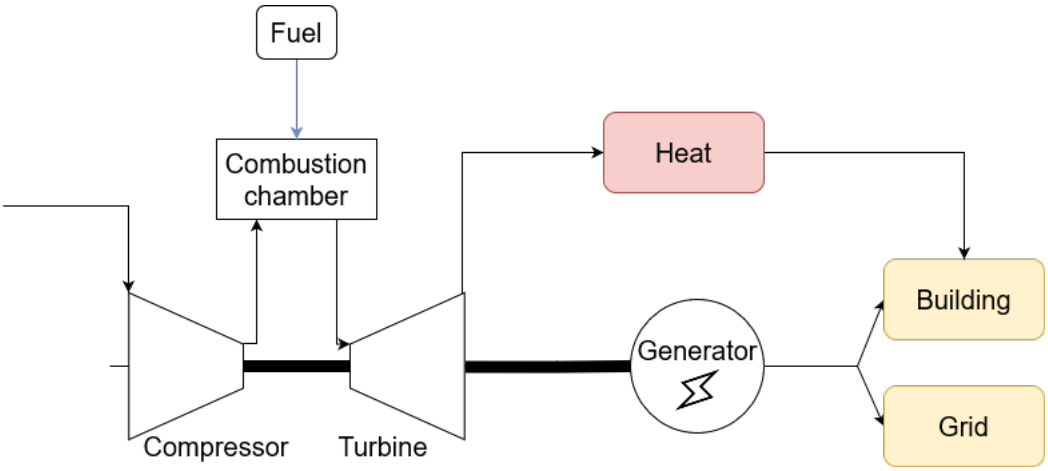

Figure 1.5: Gas turbine cogeneration

CHP based on piston engine or reciprocating engine can either be compression ignition (diesel) or spark ignition engine (petrol) [28]. It could also be adapted for other fuels, such as biofuels [29]. The advantage is that use of fossil fuel is reduced and thus reduced carbon emissions.

Steam turbine [30] use pressurized steam to convert mechanical energy into electricity and heat is generated thanks to a steam condenser. The strong point is that the steam turbine is very flexible.

The nuclear power plant [31] generates a huge amount of heat by nuclear fission to produce steam and electricity through a steam turbine. It is possible to extract 10 MWth for every MW electricity lost with a heating system of 95°C [29].

Some types of fuel cell can also be considered as CHP. Fuel cells are an electrochemical device in which a spontaneous reaction occurs [32] that produces electrical

power. These reactions are exothermic and therefore release heat. For example, molten carbonate fuel cells (MCFCs) operate at a high temperature, operating at around 650 ° C. This means that high-quality heat is available for cogeneration.

Renewable sources can be adapted to CHP. Indeed, biomass, geothermal energy, and solar thermal energy could generate both electricity and heat [33].

Micro combined heat and power or mCHP is an application of CHP for a range of up to 50 kWe in EU [26]. A micro-CHP can first meet the heat demand and produce electricity as a by-product or vice versa.These small power plants are used in particular in buildings, where the heat can be used to supply the buildings or recharge the heat storage tank.

1.3 Master thesis objectives

This master's thesis was carried out during an internship at *Mitis*. *Mitis* is a company whose main purpose is to contribute to emission reductions by developing high efficiency energy systems. Their main machine is a microturbine that has $<$ 10 ppm of NOx emissions, a high maintenance cycle, and the use of natural gas. Its main features are a global efficiency of 86 %, 10 kWe of electrical power and 40 kWth of thermal power. The purpose is to provide heating, cooling and power for public or private buildings and constitute an off-grid power solution.

As part of a project of *Mitis* called Flaminco, heat pumps are also one of the company's research. Flaminco is a machine that assembles a gas turbine feeding a heat pump and a condensing boiler.

This master's thesis aims to analyze experimentally the third version of an air-to-water heat pump with propane R290 as a working fluid. The heat pump is approximately 12 kWth of thermal power. The purpose of the machine is its commercialization or integration into the Flaminco project. Thus, it is important to study its performance according to parameters such as outdoor temperature, water temperature and compressor speed.

The second objective is to study a system composed of a condensing boiler, the mCHP, a storage tank, and a known load with a simulation tool named *Dymola*.

1.4 Overview

The document is organized as follows :

- Chapter 1 : Introduction provides a climatic and political context on heating systems and refrigerant.
- Chapter 2 : Test bench description explains how the machine is arranged, including the different parts and the data measurement.
- Chapter 3 : Experimental results shows the performance of the heat pump in different working point.
- Chapter 4 : Heat pump model and study case present the *Dymola* model and a case study.

Chapter 2

Test bench description

The heat pump test bench made available by *Mitis* is installed in the university laboratory of Liege located in Montefior in Sart-Tilman. The test machine is outside and is made up of the heat pump itself with a refrigerant loop and a water-glycol loop to simulate the user side. Figure 2.1 is a schematic of the whole system. The machine is the third version of a heat pump already studied by *Mitis*, improving the test rig at each step.

The following sections give a complete explanation of all parts.

2.1 Refrigerant circuit

The refrigerant circuit is represented in dark blue in Figure 2.1. It is made up of two heat exchangers, a compressor, an electronic expansion valve, a liquid receiver, a filter drier, and a four-way valve. One can do the analogy with picture 2.2a and 2.2b. The corresponding numbering of the images is detailed in Table 2.1. Four arrows are also drawn in Figure 2.2a to represent the one way valves which constitute a Wheaston's bridge.

For the following, "condenser" names the heat exchanger where the condensation take place and "evaporator" for the one where the evaporation take place, depending of the mode of the heat pump.

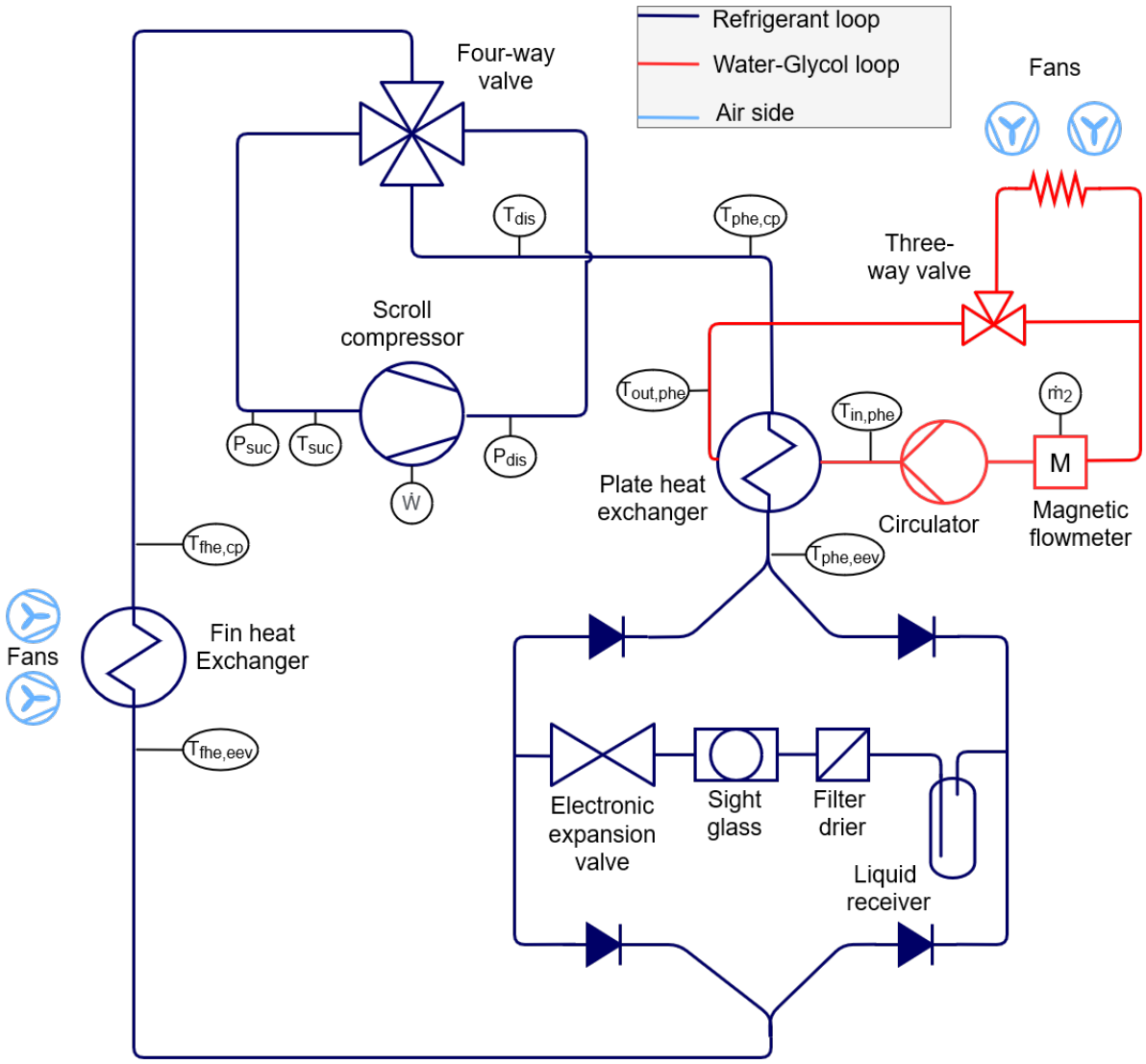

Figure 2.1: Diagram of the test bench

2.1.1 Four-way valve

As stated above, a heat pump could work in heating or cooling mode depending on the situation. In winter, the machine is used to heat up the load, while in summer it is the opposite. A problem could also happen in very cold conditions: frost could form between the evaporator fins and block the air, and thus reduce the heat exchanger surface area. A four-way valve is therefore added to allow the system to be reversible and defrost the fin heat exchanger when needed, and to produce either cold or heat. The

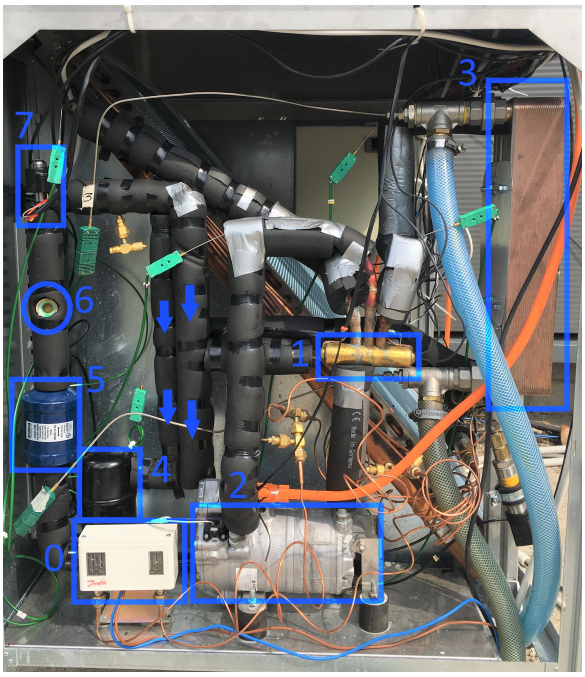

(a) Refrigerant side

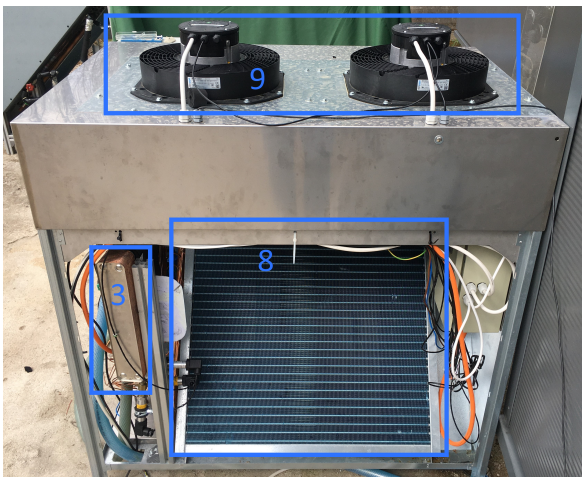

(b) Air side

Figure 2.2: Experimental set-up of the heat pump

Numbering	Component
0	Safety switch
1	4-way valve
2	Compressor
3	Plate heat exchanger
4	Liquid receiver
5	Filter drier
6	Slight glass
7	Electronic expansion valve
8	Fin heat exchanger
9	Fans

Table 2.1: Heat pump component numbering corresponding to the Figure 2.2

refrigerant circulates in one direction or the other in the heat exchangers but always in

the same way in the rest of the circuit. Thanks to the four-way valve, the heat pump usage time is increased and can be used in many outside conditions.

The four-way valve is manufactured by *SAGinoMIYA* (STF-H type). Inside the four-way valve, there is a moving solenoid pilot valve with a coil that can be controlled to change the direction of the refrigerant flow, as shown in Figure 2.3.

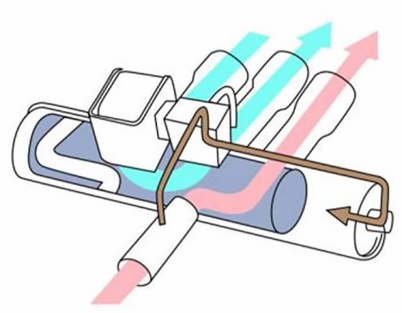

Figure 2.3: Diagram of the four-way valve. Source: [34]

2.1.2 Compressor

The compressor is a scroll-type compressor manufactured by *Sanden*, and is the fourth generation of the SHS33 model. It is a electric semi hermetic compressor which means that the motor and the compressor are enclosed in a same confined space. The sealing must then be correct and offer the possibility to be repaired in case of failure. It was designed to work at a wide range of speed: 700 RPM to 8500 RPM. The compressor is equipped with an inverter converting AC to DC to control the rotational speed and therefore the thermal load. The compressor is normally suitable for the R134a and R1234yf refrigerant. The manufacturers adapt their compressor and oil to be compatible for propane as well. The oil is used to lubricate the compressor. The oil is circulating in the refrigerant loop since there is no oil separator at the outlet of the compressor. The downside is that it decreases the heat exchanged in the heat exchangers but adding an oil separator would increase installation cost and system complexity.

The displacement of the compressor is 33 cm^3.

2.1.3 Plate heat exchanger

The heat exchanger on the load side is a brazed plate heat exchanger (BPHE) manufactured by *SWEP*. It transfers heat between the water on the user side and the refrigerant. The secondary fluid is water mixed with 30 % of ethylene glycol. It is a counterflow heat exchanger. The main advantages of the BPHE are its compactness, its efficiency, its reliability and it is cost-effective.

In heating mode, this exchanger is where the refrigerant condensation phase takes place. In cooling mode, the refrigerant evaporates in it.

2.1.4 Liquid receiver

A liquid receiver is a buffer and storage tank for liquid refrigerant. It is placed right after the "condenser" in the liquid line, as shown in Figure 2.1. An immersion tube at the bottom of the bottle draws the refrigerant and ensure it to be liquid. The amount of liquid in the receiver will vary depending on the outdoor and ambient temperature and the saturation temperature at the condenser. Its purpose is to stabilize the refrigerant charge fluctuations, to prevent the liquid from stagnating in the "condenser" or to store refrigerant in case of maintenance in the system. In fact, when the heat pump unit is changed, the refrigerant should be removed before any cleaning. This can be done by closing the liquid receiver outlet and run the compressor to push the refrigerant into the tank.

The liquid receiver is a buffer. To cover the widest operating range, the refrigerant charge must be well adjusted. In fact, if the system is overcharged, the refrigerant accumulates in the "condenser" and increases the subcooling, increasing the amount of liquid in the heat exchanger. Therefore, the efficiency of the "condenser" decreases since the heating capacity of a liquid is lower than that of a diphasic mixing. On the contrary, if there is not enough refrigerant, the overall gaseous phase will increase throughout the circuit and the expansion valve could no longer be in the liquid phase, causing a malfunction. Due to the liquid receiver, refrigerant can be stored in case of overcharged system and released in the opposite case.

However, the liquid receiver requires an additional refrigerant charge to be partially filled at any time and also constitutes an increase of the cost of the heat pump and its complexity.

The liquid receiver used in the test bench is from *denaline s.p.a.* and has the

characteristics of Table 2.2

Volume [L]	0.7
Maximum permissible pressure [Bar]	30
Temperature range [°C]	-10/+100

Table 2.2: Technical data of the liquid receiver from *denaline*

2.1.5 Filter drier

A bidirectional filter dryer is added in the liquid line between the liquid receiver and the expansion valve. It is manufactured by *DENA* and is compatible with most of the refrigerant. This device protects the refrigerant and the plant from any kind of pollution. The filter effectively prevents any impurities from flowing back. The filter captures and absorbs water particles as well as harmful solid particules. This will prevent them from cycling around the circuit and entering the compressor, expansion valve, etc., and keep the system running in optimal condition.

2.1.6 Electronic expansion valve

An electronic expansion valve (EEV) is used to control the refrigerant flow in precise amounts. By moving up and down a needle, it decreases the pressure of the fluid and partially vaporizes it, and thereby controls the superheat at the "evaporator". Refrigerant flow rate regulation is a sensitive task. If the refrigerant flow is too small, it could cause a consequent rise in temperature. This means that the efficiency of the evaporator would decrease as a result of the warm-up and overheating of the refrigerant. Moreover, excessive refrigerant discharge leads to insufficient evaporation, which could damage the compressor due to residual liquid. Therefore, the EEV continuously adjust its opening to achieve optimal overheating. Then a pressure and temperature sensor is required at the compressor suction line.

An EEV is more compact, more reliable, more precise and more reactive than a thermal expansion valve. The efficiency of the system is therefore increased and has a better COP.

The expansion valve is manufactured by *Dansfoss* (model ETS 6). It is driven by a permanent magnet type direct operating stepper motor drive and controlled by the

EKE 1C superheat controller.

2.1.7 Wheaston's bridge

Four one-way valves or check valves are used in the liquid line to make a layout similar to a Wheaston's bridge, hence its name. A one-way valve is a valve that allows fluid to flow through it in one single direction, exactly like a diode in an electrical circuit. This device is a *Danfoss* product type NRV.

This configuration is useful for the heat pump to be reversible. As already mentioned in Section 2.1.1, the heat pump could work in the heating mode or in the cooling mode, depending on the position of the four-way valve. Two situations are then possible for the bridge. Figure 2.4a and 2.4b illustrate both case with a more simple drawing of the bridge. The green arrow shows the direction of the refrigerant. Pressure has to be taken into account when looking at the path. In fact, in Figure 2.4a, the flow could pass through valve 1 after the expansion valve, but since the pressure is higher at the condenser outlet, this would never be the case. In this way, the refrigerant always flows in the same direction in the expansion valve but flows in one way or the other in the heat exchangers, depending on the mode of the heat pump.

2.1.8 Fin heat exchanger

The air heat exchanger is a plate-fin heat exchanger (PFHE) and transfers heat between the refrigerant and the outside air. Since air has a lower specific heat than water, this heat exchanger requires a larger area, and constitute the largest part of the heat pump. The tubes, headers, and connectors are made of copper, and fins are made of aluminum. In Figure 2.2b, it can be seen that the evaporator is inclined. It allows to gain place, without affecting the airflow created by the fans. In fact, the components visible in Figure 2.2 are normally covered with a metal plate so that the air flow can only come from the bottom of the heat exchanger and also protect the various devices (see Figure 2.5) from rain.

2.1.9 Fans

Two axial fans are added on top of the heat pump to create roughly constant airflow in the evaporator. They are manufactured by *ebmpapst* and their main technical data

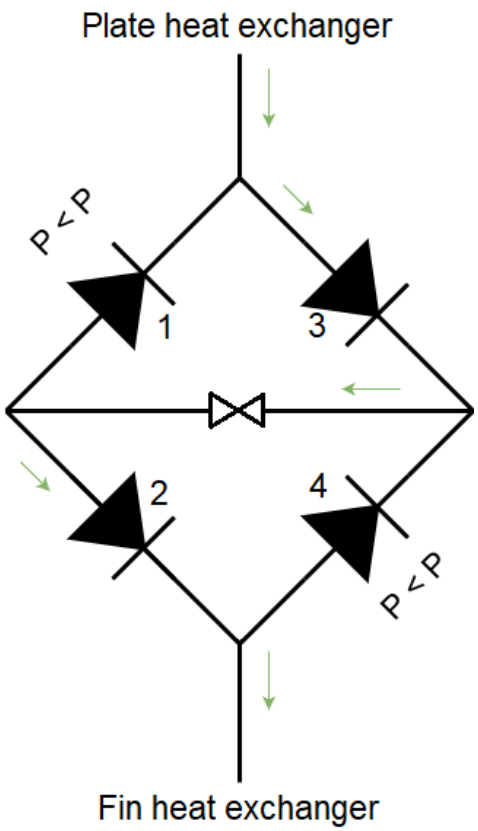

(a) Wheaston's bridge in heating mode

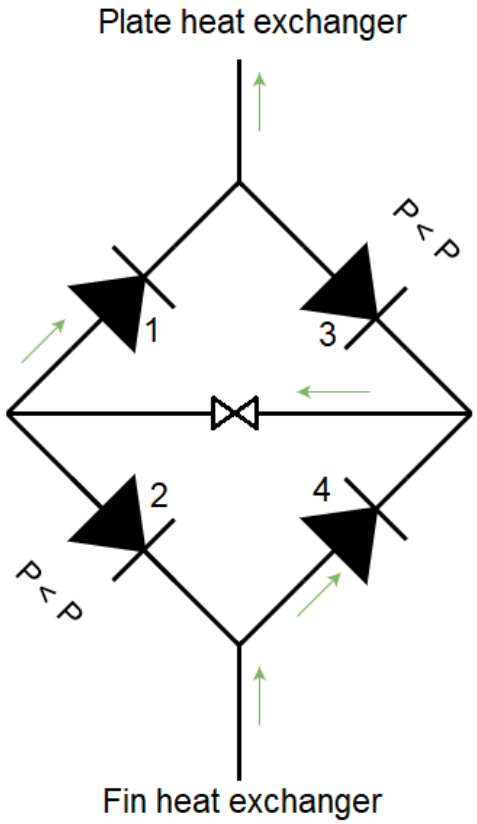

(b) Wheaston's bridge in cooling mode

Figure 2.4: Path of the refrigerant on the Wheaston's Bridge

at nominal point are listed in the table 2.3.

Model	W3G300-ZG06-01
Voltage (AC) [V]	230
Speed [RPM]	2520
Power input [W]	340

Table 2.3: Nominal technical data of the axial fans

Figure 2.5: Picture of the heat pump

2.2 User side

The user side is represented in red in Figure 1.2. To study the heat pump at different working points, the user side is replaced by a hydraulic loop connected to the plate heat exchanger, where the heat is useful. Ethylene glycol is added to the water at a concentration of thirty percent to prevent the circuit from freezing when it is cold. The flow rate is controlled by a circulator and a magnetic flow meter. The thermal load is modeled by an air-to-water heat exchanger, releasing the heat to the outside air thanks to two fans. A three-way valve adjusts the temperature at the heat exchanger terminal, bypassing the thermal load more or less as shown in Figure 2.1. Figure 2.6 shows the component of the secondary loop composed of the pump (1), the magnetic flowmeter (2) and the 3-way valve (3).

2.2.1 Hydraulic pump

The circulator in the water loop is an E pump of *Grundfos* with a frequency-controlled motor. Table 2.4 shows its main technical data. The flow set point is chosen to have almost 5 degrees of rise in the condenser. It is driven by an electrical signal, which is converted into rotational speed.

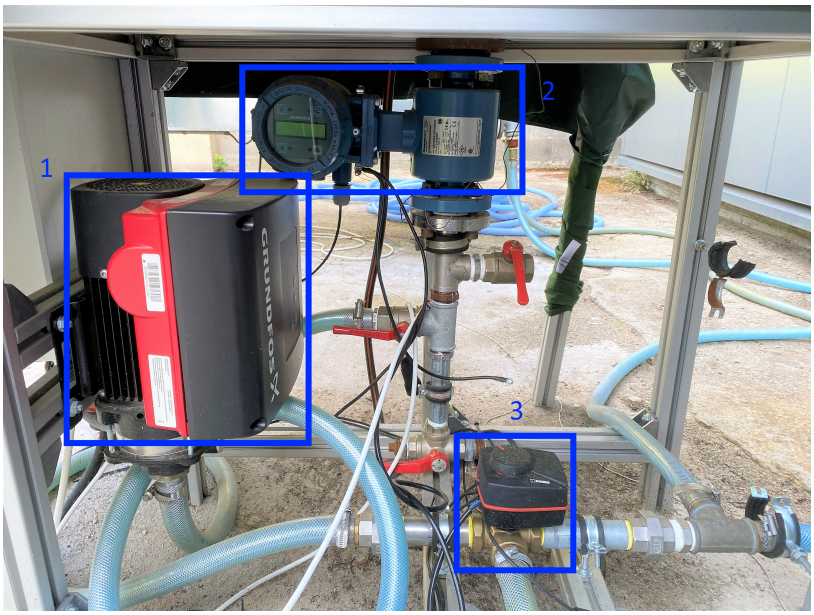

Figure 2.6: Picture of the user side of the test bench

Model	CME 5-2 A-R-A-E-AQQE S-A-D-N
Nominal flow rate [m^3/h]	5.64
Nominal power Speed [kW]	1.1

Table 2.4: Nominal technical data of the hydraulic pump

2.2.2 Three-way valve

A motorized three-way valve from *ESBE* (ARA600 model) is added to the secondary loop to control the temperature of the user side. It receives a varying tension and convert it from 0 to 10 which allows a progressive variation of its opening. 0 means that it is fully closed and the thermal load is bypassed, while 10 means that it is fully open.

2.2.3 Thermal load

The thermal load is simulated by a heat exchanger and two fans which reject the heat transported by the water from the condenser to the outside air. This component is from the manufacturer *AIA*.

2.3 Test rig instrumentation

To study the performance of the component and the system itself, the test rig is equipped with sensors in strategic position, as shown in Figure 2.1. All the sensors are connected to a card to perform data acquisition. The communication with labview and the components is made trough NI-VISA, an application programming interface (API). Full details on sensors and data monitoring are explained in the following sections.

2.3.1 Sensors

2.3.1.1 Thermocouples

K-type thermocouples were used to measure the temperature at various points in the refrigerant circuit and the secondary loop. Generally, a thermocouple is made of two wires of dissimilar electrical conductors, forming a junction where the temperature needs to be measured. This led to a voltage dependence on temperature as a result of the Seebeck effect. Hence, when the temperature is changing, the voltage difference can be interpreted to measure temperature, using thermocouple reference table.

Table 2.5 recaptures the main aspect of K-type thermocouples.

Metals	Chromel - Alumel [1]
Temperature range [°C]	-200 +1350
Sensitivity [µV/°C]	41
Accuracy [%]	± 0.75

Table 2.5: Main characteristics of a K-type thermocouple

Table 2.6 lists the temperature sensors used and their locations. Since the heat pump could work both in heating and cooling mode, the refrigerant flow could change in the heat exchanger. Thus, the supply or exhaust line of the heat exchangers are not fixed. It is more convenient to name the thermocouples on the basis of their location.

[1] Chromel is an alloy made of approximately 90% nickel and 10% chromium by weight. Alumel is an alloy consisting of approximately 95% nickel, 2% aluminum, 2% manganese, and 1% silicon.

Measurement device	Test bench name	Location
K-type thermocouple	T_{suc}	Compressor suction line
	T_{dis}	Compressor discharge line (after four-way valve)
	$T_{phe,cp}$	Plate heat exchanger compressor side
	$T_{phe,eev}$	Plate heat exchanger EEV side
	$T_{fhe,cp}$	Fin heat exchanger compressor side
	$T_{fhe,eev}$	Fin heat exchanger EEV side
	$T_{cp,eev}$	EEV superheat control
	$T_{in,phe}$	Plate heat exchanger inlet (water side)
	$T_{ou,phe}$	Plate heat exchanger outlet (water side)

Table 2.6: List of thermocouples used on the test bench

2.3.1.2 Pressure sensors

Three pressure transducers are used for the test rig. Two of them are placed at the compressor terminals and are used to determine the saturation stages and compressor performances. The third one allows the expansion electrical valve to control the superheat. Table 2.7 summarizes the three pressure sensors. These sensors are based on the piezoelectric effect. A small piece of material is stretched and produces a signal depending on the pressure. The sensor for the EEV is from *Apilsen* model PC-28. It can measure any pressure in the range from 0-25 bar and has an accuracy of ± 0.2%. The two others are from *Keller* model 33X. They have a range from 0 to 40 bars with an accuracy of ±0.05%. The pressure sensors being quite expensive, adding more of them would not be a good idea, since an obvious objective is to reduce the cost of installation. Indeed, there are only two pressure stages, if we leave the pressure drops, which are very minimal compared to the pressure difference at the compressor and the EEV.

Measurement device	Test bench name	Location
Pressure transducer	P_{suc}	Compressor suction line
	$P_{suc,eev}$	Compressor suction line (EEV)
	P_{dis}	Compressor discharge line

Table 2.7: List of pressure transducers used on the test bench

2.3.1.3 Power meter

A power meter measures the consumption of the inverter and in this way the compressor consumption.

2.3.1.4 Magnetic flowmeter

The secondary loop is equipped with a Rosemount *Emerson* model magnetic flowmeter to precisely measure the water flow rate and then control the temperature difference in the condenser. The main technical data of this device are summarized in the table 2.8. The product consists of the transmitter where the display shows the flow rate value and the sensor where the water flows.

Model	Rosemount 8705
Range [l/s]	0 to 1.2
Flow accuracy [%]	±0.25
Transmitter accuracy [%]	±0.25

Table 2.8: Nominal technical data of the magnetic flowmeter from *Emerson*

The based principle consist of coils that generate a magnetic field. The magnetic flow meter sensor is placed inline and measures the induced voltage generated by the fluid as it flows through a pipe. The transmitter takes the voltage generated by the sensor, converts the voltage into a flow measurement, and transmits it to a control system. Their advantages are that there is less obstruction, they are cost-effective, bidirectional, and provide highly accurate volumetric flow measurement.

2.3.2 Sight glass

A sight glass is a device that allows a direct control of the state of the refrigerant and is placed as close as possible of the inlet of the expansion valve. In fact, the EEV should work with a subcooled liquid, and no bubbles should then be seen on the sight glass. It is used to check that the total mass of refrigerant in the system is sufficient. If not, the pressure is not high enough and the refrigerant could not be in a supersaturated liquid state in the condenser, and bubbles are visible on the glass.

2.3.3 Safety pressure sensor

A safety pressure sensor is mandatory in such installation. Figure 3.17 is a zoom of device 0 of Figure 2.1. Three terms are used when describing pressure switch settings: cut-in, cut-out, and differential. The cut-in pressure is the lowest acceptable pressure in the system and is equal to 0.5 bar and is measured at the compressor suction line. The cut-out pressure is fixed at 30 bars and is the maximum pressure acceptable for pipes, sensors, components, etc. to be impervious. Logically, it is connected to the compressor discharge line, where the pressure is at its maximum. Beyond this interval, the compressor is immediately stopped by a switch inside the safety switch. The differential ("DIFF" on picture) is the difference of pressure at which the compressor could be turn on again. In this case, the compressor will only be able to start once the pressure has dropped to 27.75 bars.

2.3.4 Data management

Data management is permanently performed between LabVIEW and a microcontroller through VISA communication. Thus, the various actuators of the heat pump can be controlled and the sensors studied.

2.3.4.1 Microcontroller

An electronic breadboard is created by *Mitis* to allow communication between a microcontroller and measuring devices, as well as the electronic component of the test bench that can be controlled. The microcontroller is manufactured by *STMicroelectronics*. Its use is very convenient because it connects to the computer via a single USB cable and allows many operations.

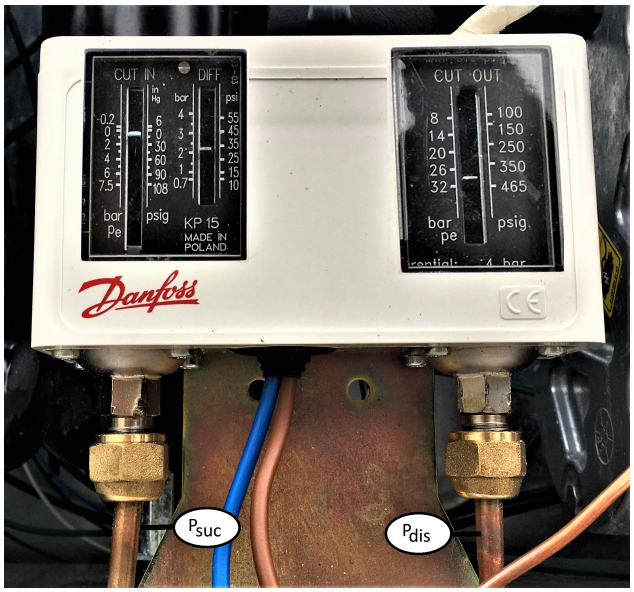

Figure 2.7: Picture of the safety pressure sensor

2.3.4.2 Visa

VISA communication is an NI product (*National Instruments*) that provides a programming interface to control a USB device in an NI application such as LabVIEW. Each 0.25 seconds, a group of data is exchanged with the microcontroller. Some commands are defined with "#" and letters followed by numbers, translated by the microcontroller, to give instructions to the devices.

2.3.4.3 LabVIEW

LabVIEW is a platform for designing measurement and control systems, based on a graphical development environment from *National Instruments*. It is a VI (Virtual Instrument) which means that, it is possible to follow in real time the evolution of the system. Fans, compressor speed, 3-way valve opening are directly controlled in LabVIEW.

Some calculations are performed directly in LabVIEW such as coefficient of performance, TS chart, etc. via sub-VIs calling python code. The results are stored every second in a .txt file and have been postprocessed in Matlab.

Chapter 3

Experimental results

The heat pump has been tested for several working points. The experimental part is mainly focused on the heating mode of the machine. This chapter presents the results of the test campaigns and post-processing. The heat pump is the third version of a test bench. From the above, it appears that a total mass of 1 kg of propane gives good results and good behavior to the machine.

3.1 Equations

The experimental results are studied through equations which give the performance of the system. Indices are listed in the nomenclature section. The compressor, heat exchangers, coefficient of performance, and mass flow rate of refrigerant are studied. All the data are studied with Matlab and using the CoolProp library, which allows to calculate the state of the refrigerant.

3.1.1 Refrigerant mass flow rate

Since there is no mass flow rate measurement device for the refrigerant loop, the propane flow rate $\dot{m}_r$ has to be estimated by some calculations based on the thermocouples and the magnetic flow meter. The heat exchanged on the user side of the plate heat exchanger can be calculated using equation (3.1). The heat exchanged $Q_{w,phe}$ is given by:

$$\dot{Q}_{w,phe} = \dot{m}_w.c_p.(T_{in,phe} - T_{out,phe}) \tag{3.1}$$

where c_p specific heat capacity of water

It is assumed that heat is totally transferred between water and refrigerant (3.2), then equation (3.3) can be calculated and the refrigerant mass flow rate is estimated.

$$\dot{Q}_{w,phe} = \dot{Q}_{r,phe} \tag{3.2}$$

$$\dot{Q}_{r,phe} = \dot{m}_r.(h_{phe,cp} - h_{phe,eev}) \tag{3.3}$$

where $h_{phe,cp}$ - $h_{phe,eev}$ is the difference in refrigerant enthalpy at the plate heat exchanger. Those equations are valid for both modes of the heat pump, since (3.1) and (3.3) are both positive in the heating mode or negative in the cooling mode.

3.1.2 Compressor

The performance of a compressor is studied through its volumetric and isentropic efficiency, calculated by equation (3.4) and (3.7). By definition, volumetric efficiency is the ratio between the volumetric flow rate of the fluid displaced by the scroll compressor $\dot{V}_{r,suc}$ and the actual displacement of the scroll $\dot{V}_{r,th}$. In fact, the difference between the two comes from a leak.

$$\epsilon_{vol} = \frac{\dot{V}_{r,suc}}{\dot{V}_{r,th}} \tag{3.4}$$

The theoretical volumetric flow rate is given by

$$\dot{V}_{r,th} = \frac{N.V_s}{60} \tag{3.5}$$

with N the rotational speed in RPM and V_s the swept volume and the actual volumetric flow rate.

$$\dot{V}_{r,suc} = \frac{\dot{m}_r}{\rho_{r,suc}} \tag{3.6}$$

The isentropic efficiency is in theory the ratio between the isentropical work and the real work done by the compressor. From a practical point of view, the electrical consumption of the compressor $\dot{W}_{cp,elec}$ is taken into account. Indeed, it is more practical to introduce the loss made by the conversion from AC to DC, the thermal loss, and the isentropic loss in the efficiency calculation.

$$\epsilon_{is} = \frac{\dot{m}_r(h_{r,dis,is} - h_{r,suc})}{\dot{W}_{cp,elec}} \tag{3.7}$$

where $h_{r,dis,is} = f(s_{r,suc}; T_{phe,cp})$ is the discharge enthalpy for an isentropic compression.

3.1.3 Heat exchanger

The plate heat exchanger equations are the following, where $\dot{Q}_{w,phe}$ is given by (3.3) and $\dot{Q}_{r,phe}$ by (3.1).

$$\dot{Q}_{phe} = \dot{Q}_{w,phe} = \dot{Q}_{r,phe} \tag{3.8}$$

3.1.4 System performances

The coefficient of performance (COP) of the machine is given by the useful work divided by the work provided:

$$COP = \frac{\dot{Q}_{phe}}{\dot{W}_{cp,elec} + P_{fans}} \tag{3.9}$$

This value characterizes a machine in heating mode. The equivalent ratio in cooling mode is called the energy efficiency ratio (EER):

$$EER = \frac{\dot{Q}_{phe}}{\dot{W}_{cp,elec} + P_{fans}} \tag{3.10}$$

3.2 Experimental analysis

The heat pump has been tested outside at the university and during two months. The experimental campaign is made of 57 results. They have been recorded in steady state of the heat pump. Because the outside temperature cannot be controlled and since it changes quite quickly, the steady state is not fully reached. Thereby, the recording is made during roughly 5 minutes and all the calculations are made with the average of each measurement. This allows to reduce measurement noises and to dampen the variation of the external temperature and system oscillation. The heat pump was tested under the widest possible conditions. The mass flow rate of the water is chosen

to provide a temperature difference of 5 ° C on the plate heat exchanger. The water-glycol outlet temperature $T_{out,phe}$ is varied from 35 ° C to 60 ° C with a step of 5 ° C. The range of temperature is chosen to reproduce a hot water point for a heating device. The low temperature 35 ° C is more for floor heating and the high temperature 55 ° C-60 ° C for radiators. The temperature of hot water is limited by the maximum pressure allowed in the refrigerant circuit by the safety switch. For certain particular points, by hot outside air and high compressor speed, the maximum reachable temperature decreases.

The heat pump ran for different outside temperatures: 10 ° C, 12 ° C, 14 ° C, 16 ° C, 19 ° C, 20 ° C, and 22 ° C. Thus, the heating and cooling modes could be recorded and the heat pump could be characterized for most European regions. As the test campaign took place in April and June, the temperature was not so low.

The compressor speed is another parameter and is fixed at 4000, 5000, 6000 and 7000 RPM. Note that when the saturation temperature at the plate heat exchanger is too high, the compressor could not reach the set point and the rotational speed decreases due to a too high pressure difference.

Due to technical problems on the test bench, the first tests was not truly representative. The connection of the USB cable for data acquisition is not reliable and the ground is somehow not connected which conducts to wrong reading of the pressure sensor.

All actuators are manually controlled in the labview VI interface, trough the VISA communication.

All the figures in the following sections refer to the sensor names previously defined in the Table 2.6 and 2.7.

3.3 Heating mode

First, the heat pump was tested in heating mode, i.e. the water is heated by drawing in heat from outside. The condensation of the refrigerant takes place in the plate fin heat exchanger and the evaporation in the fin heat exchanger. Regarding the heat load, the study is more concentrated on the plate heat exchanger, since the useful heat is exchanged there.

Figure 3.1 shows the points obtained during the whole test campaign and the pressure ranges.

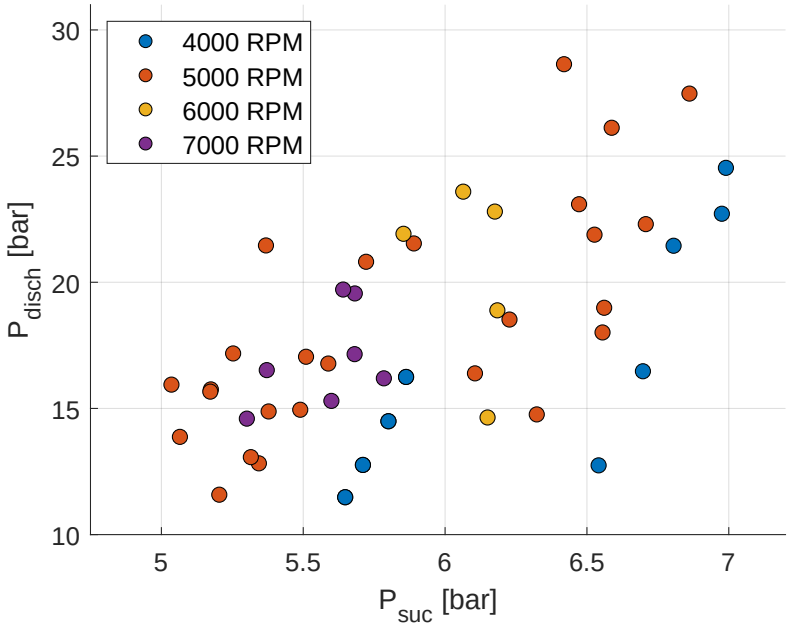

Figure 3.1: Tests results in heating mode of the whole test campaign

3.3.1 Validation of measurements

Any measurement analysis should take into account the inaccuracy of the sensors, the communication bus, and the uncertainty of all devices of the heat pump. This could cause bad results and a bad translation of the behavior of the machine. Therefore, it is important to verify the results from a global point of view and to exclude bad tests or bad sensor measurements.

As already indicated, all results are analyzed as an average value over 5 minutes of testing, but reading errors could distort these average values. Figure 3.2 shows the pressure measured at the suction and discharge line of the compressor during one of the tests. It seems like the discharge reading oscillates between two values, 19 and 15 bars, while the suction pressure is stable at 6 bars. This error happened for most of the test and the oscillation should be filter. The discharge pressure is a key measurement when characterizing the heat pump. The saturation states, compressor efficiency, refrigerant mass flow rate, and system performance are affected by pressure, so special attention should be paid to this sensor measurement. Now the problem is to know which value is the actual one.

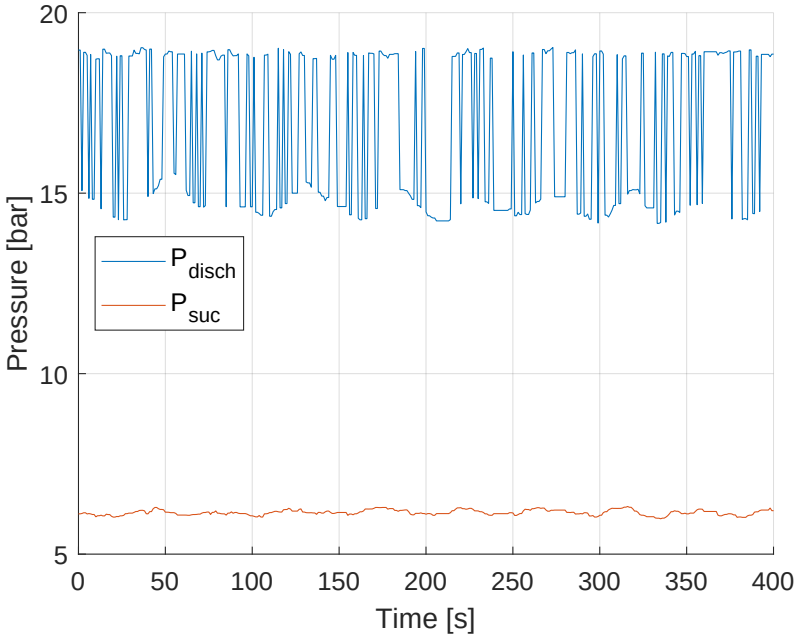

Figure 3.2: Reading of the pressure sensor during one of the tests

The temperature entropy diagram in Figure 3.3 could give a good indication. The T-S diagram is represented twice consecutively, where the pressure increases from 14,5 bars to 18,5 bars at once. The blue cycle seems to be correct and shows a classical T-s diagram, as shown in the introduction in Figure 1.3. The orange bar clearly shows that the cycle based on the $P_{disch} = 18,5$ bars is impossible. Indeed, the entropy at the supply of the plate heat exchanger (also the discharge of the compressor), which is calculated in function of the discharge pressure and the discharge temperature, shows that the compression is losing entropy, which is clearly an error. Another indication is that the saturation level[1] of the orange cycle in Figure 3.3 in the exchanger is above the compressor exhaust temperature T_{dis}, which is impossible because the ambient temperature is lower. The problem could only come from the pressure sensor since the temperature sensor was quite stable throughout the test, as shown in Figure 3.4. This figure gives the discharge temperature, the supply temperature of the plate heat exchanger, and the calculated saturation temperature inside the exchanger as a function of time for the exact same test as in Figure 3.2. The oscillations of T_{disch} and $T_{phe,su}$ are just system oscillations, while the saturation temperature bugs the same way as the pressure. Once again, it is clear that the saturation temperature is sometimes higher

[1] As a reminder, the saturation levels are represented by the horizontal lines

than the supply temperature, which supports the fact that the measured pressure is erroneous at some time steps.

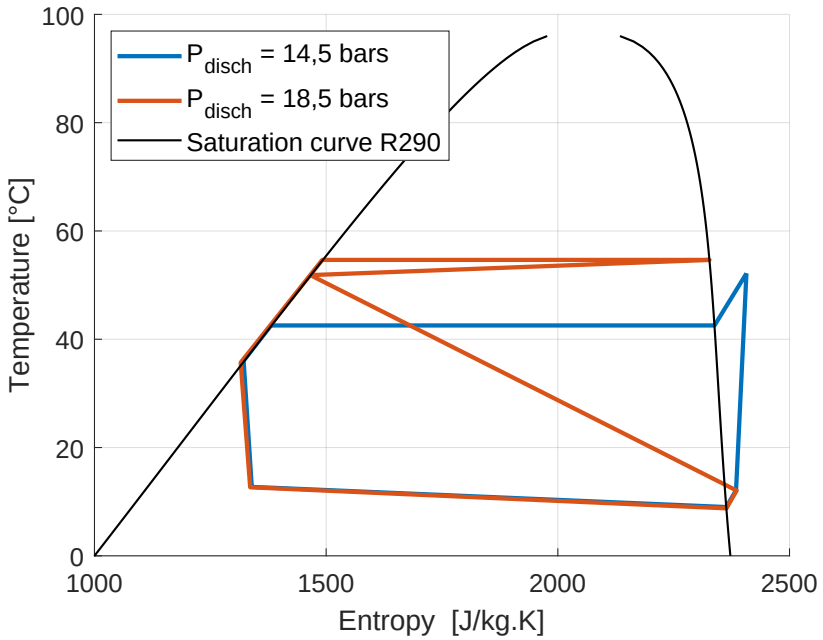

Figure 3.3: T-s diagram of the refrigerant cycle for time step 347 and 348 of one of the test

As a result, since an average is made over time for all tests, the time steps that present inconsistencies such as those of the figures 3.2, 3.3 and 3.4 has been removed to filter the pressure measurement.

The sensor T_{disch} also had some bad reading or bad connection for some tests, as shown in Figure 3.5. Normally, the difference between T_{disch} and $T_{phe,su}$ should be positive and close to zero. The difference comes from a heat loss in the four-way valve. For instance, tests 35 to 37 show some errors, where T_{disch} equals -999 K.

Figure 3.6 shows a comparison between the calculated compressor consumption and the measured consumption at the inverter. Consumption is calculated in two ways: equations (3.11) and (3.11) calculate the actual work done on the refrigerant, based on T_{disch} or $T_{phe,su}$.

$$\dot{W}_{calculated} = \dot{m}_r.(h_{disch} - h_{suc}) \tag{3.11}$$

$$\dot{W}_{calculated} = \dot{m}_r.(h_{phe,su} - h_{suc}) \tag{3.12}$$

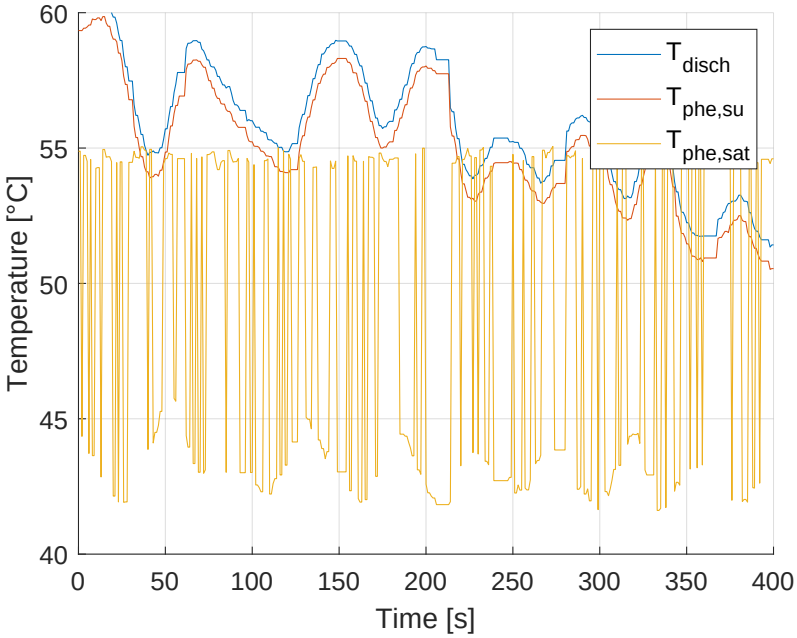

Figure 3.4: Reading of the temperature sensors T_{disch} and $T_{phe,su}$ of one of the tests

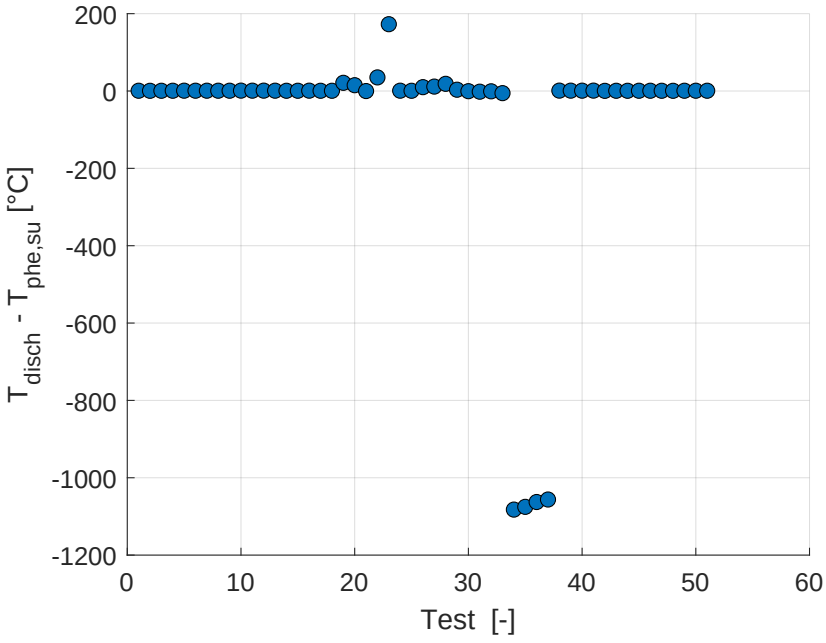

Figure 3.5: Difference of temperature between sensors T_{disch} and $T_{phe,su}$

In Figure 3.6 (a) and (b), the calculated consumption should never exceed the measured one, since there are losses in the inverter and in the compressor. In other words, the

blue point should never be below the dark line in the Figures. This shows again that for some tests, T_{disch} is not reliable. Thus, it is chosen to use $T_{phe,su}$ for all analysis of the heating mode.

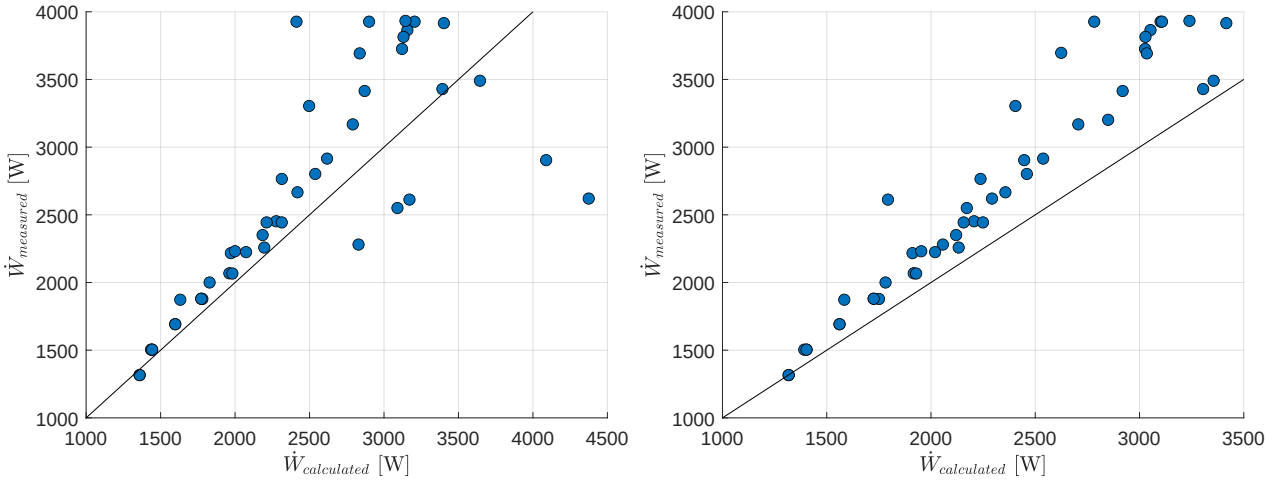

(a) (b)

Figure 3.6: Comparison of the compressor's consumption measured at the inverters and calculated by the enthalpy difference based on T_{disch} (a) and $T_{phe,su}$ (b)

It is also important that the machine is impervious, that it has the longest possible lifespan, and also that it does not distort the experimental campaign, since it lasted 2 months. The exact same test has been performed at 4000 RPM, at an outside temperature of 14 ° C. Figure 3.7 shows the tests for several water temperature. The COP did not change during the one-month interval, which is very positive.

The rotation speed of the compressor can also be limited at certain operating points. For example, Figure 3.8 is a test at $T_{out,phe} = 60°C$ and $T_{air} = 20°C$. The setpoint of the rotation speed was 6000 RPM, but when the discharge temperature increases during the transient phase, the rotation speed gradually decreases, because it is more difficult to compress hot gas. It was decided to remove tests where the rotational speed it not at the set point.

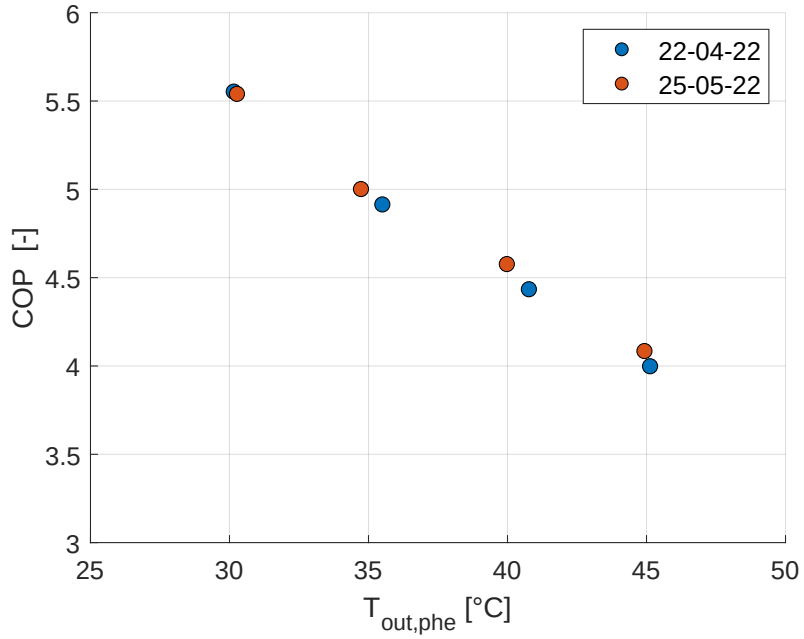

Figure 3.7: Evolution of the cycle performances over one month in function of the water-glycol temperature

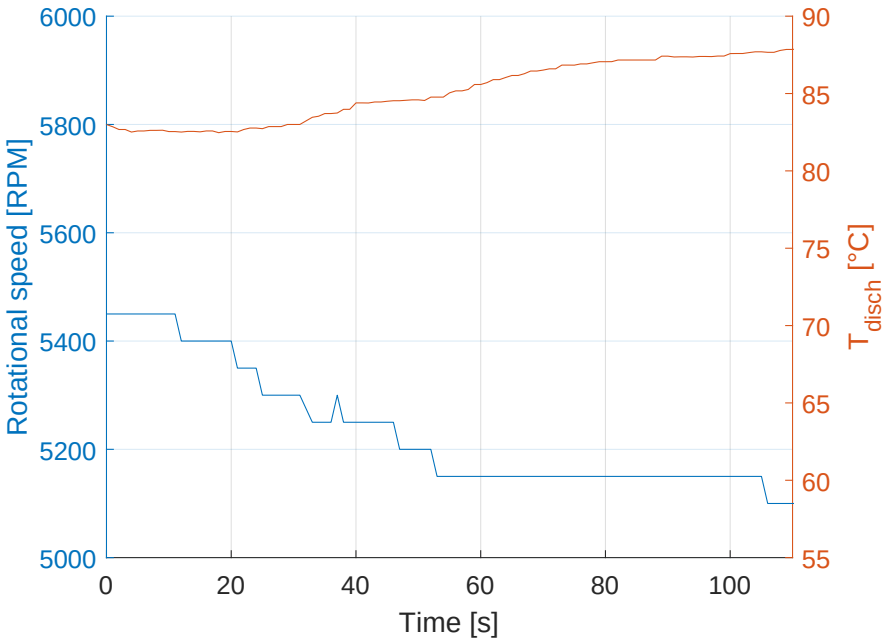

Figure 3.8: Rotational speed ceiling at $T_{out,phe} = 60°C$ and $T_{air} = 20°C$

3.3.2 Refrigerant mass flow rate

Since there is no mass flow rate measurement device for the refrigerant loop, it has to be estimated by equation (3.3). Indeed, the efficiency of the compressor depends on the flow rate. Note that this calculation does not take into account the heat loss in the plate heat exchanger and assumes that it is adiabatic. The refrigerant mass flow rate is represented in Figure 3.9 for all tests. It is clear that the mass flow increases with the rotational speed of the compressor, which was predictable by the equation (3.5).The value ranges from almost 0.03 kg/s to 0.05 kg/s, which is plausible with respect to the total refrigerant mass of 1 kg. The previous version of the heat pump, the study of which was led by Sophie Mullender [35], gave a similar total mass-mass flow ratio: 5.24 kg for a flow rate ranging from 0.1 kg / s to 0.3 kg / s at 50-60 Hz. The following discussion will show that the mass flow rate is not really reliable.

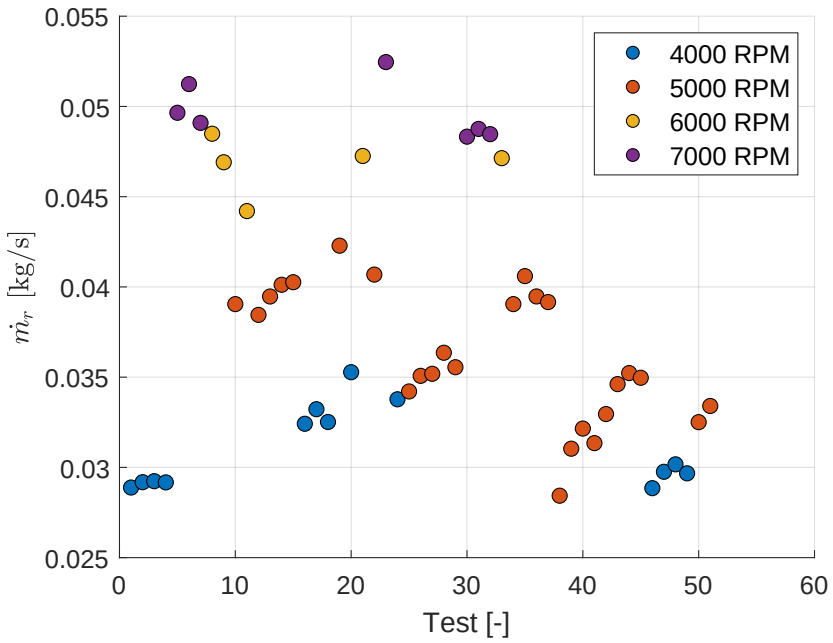

Figure 3.9: Estimation of the refrigerant mass flow rate of the database

3.3.3 Compressor performance

The compressor performance is studied through its isentropic and volumetric efficiency, described by equation (3.7) and (3.4) respectively. Their dependence on water temperature, air temperature and rotational speed are shown.

Figure 3.10 (a) illustrates the calculated isentropic efficiency as a function of the pressure ratio of the entire test company. The efficiency is maximal when the pressure ratio is lower around 2 and at low rotational speed at 4000 RPM. It varies from 0.68 to 0.9, with a mean value of 0.79. These values are, of course, overestimated, since the mass flow rate is estimated and not taking into account the losses in the plate heat exchanger. Figure (b) shows that ϵ_{is} is higher for lower mass flow, which is counterintuitive with respect to equation (3.7). Especially visible in Figure 3.10 (a), it seems like a point is drawing curves. Variation in efficiency is huge when the pressure ratio or mass flow rate is constant. Moreover it cannot be concluded that ϵ_{is} increases continuously with rotational speed since some points at 4000RPM are below some at 7000RPM. Thus, there is somehow a dependency on other parameters.

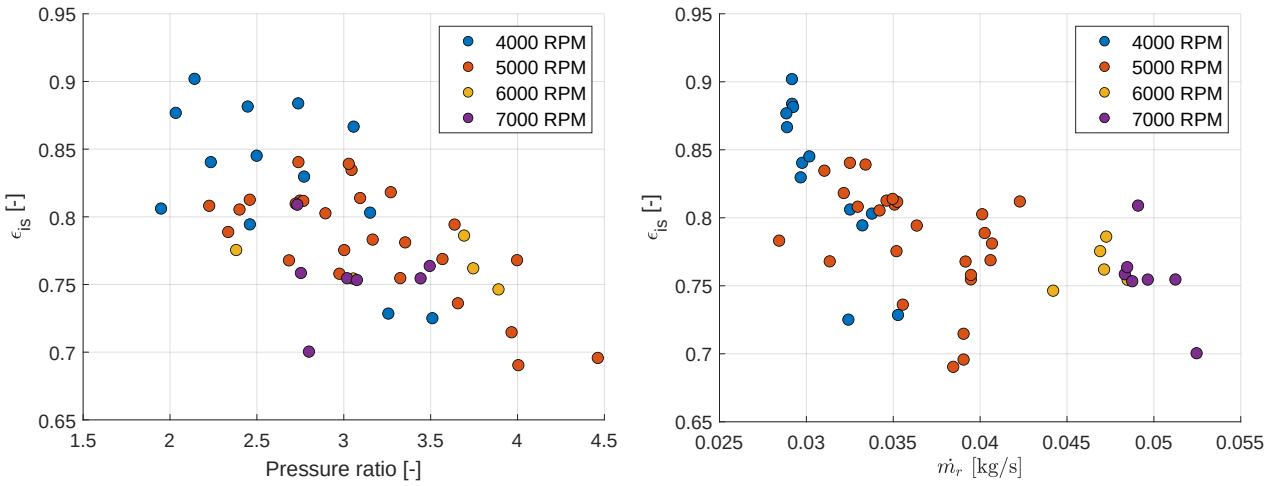

(a) (b)

Figure 3.10: Compressor isentropic efficiency in function of the pressure ratio (a) and the refrigerant mass flow rate (b)

When looking at the tests at 5000RPM, the influence of water temperature and air temperature appears. Figure 3.11 (a) clearly shows that the efficiency of the compressor decreases when the outside temperature increases. The compressor is also more efficient at low water temperature. From a practical point of view, this compressor will be more useful for a heat pump for underfloor heating. The good thing is that the heat pump in heating mode is not really needed when the air temperature increases, and then the compressor can be at the optimum often enough. Figure (b), which is a test at fixed

water (45°C) and air temperature (14°C), confirms that the efficiency decreases when increasing the rotational speed.

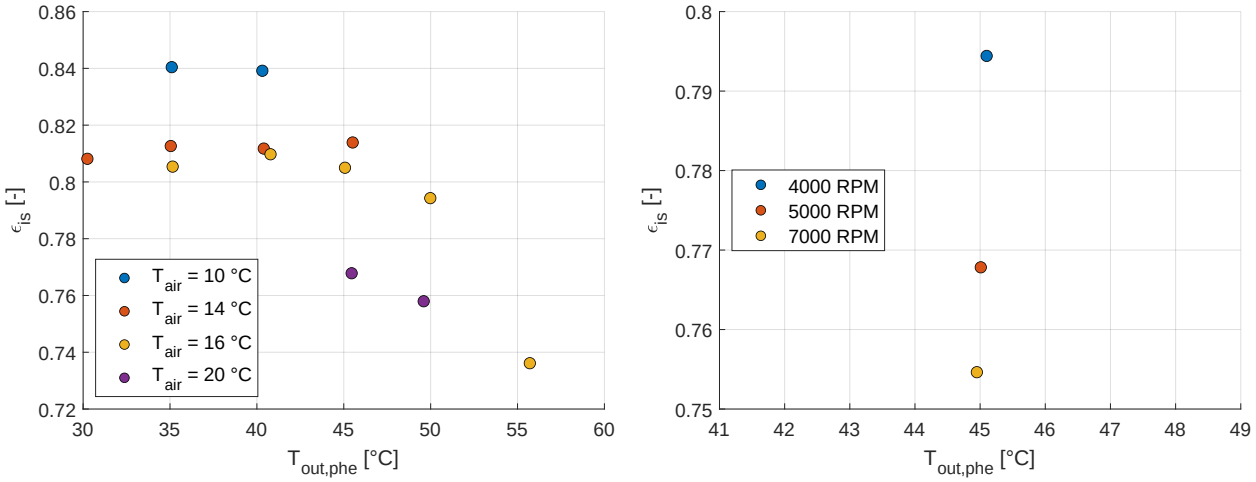

(a) (b)

Figure 3.11: Compressor isentropic efficiency in function the air temperature and the water temperature (a) and the rotational speed (b)

The volumetric efficiency described by equation (3.4) gives impossible results. Indeed, in Figure 3.12 (a) and (b), the volumetric efficiency is greater than 100% which would mean that the compressor pushes more refrigerant than the movement of the scroll itself, which is strictly impossible. The problem probably comes from the estimation of the mass flow, especially from the assumption that the plate heat exchanger is adiabatic. Thus, ϵ_{vol} is overestimated, same for ϵ_{is}. What can be seen is that the volumetric efficiency is maximum for lower pressure ratio which is understandable. In fact, when the pressure difference is increased, the leakage in the scroll compressor inevitably increases. Figure 3.12 (b) shows that the volumetric efficiency is globally higher when the mass flow is greater.

3.3.4 Cycle performance

The cycle performance is quantized by its coefficient of performance (COP). It is one of the most important indicators for the ranking of the heating system. It is calculated by equation (3.9), which is the ratio of heating capacity to power consumption. The

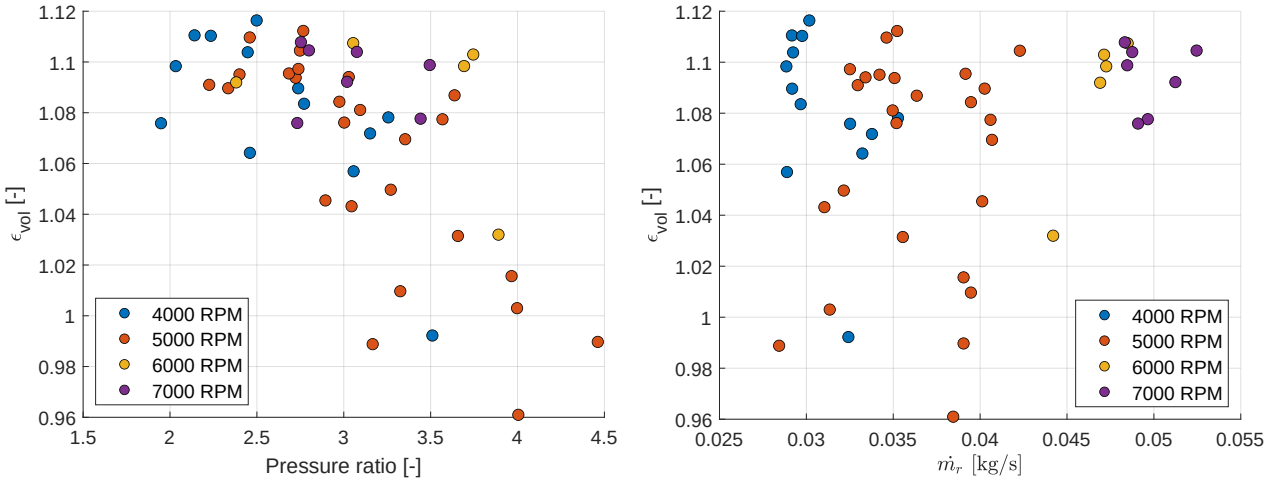

(a) (b)

Figure 3.12: Compressor volumetric efficiency in function of the pressure ratio (a) and the refrigerant mass flow rate (b)

consumption of the inverter is taken into account to introduce also all the losses of conversion in the calculation of the COP.

Figure 3.13 (a) highlights the influence of water temperature and air temperature on COP. This is important to know since those two parameters are external to the machine. The heat pump is more efficient at low water temperature and at high outside temperature. Again, the machine is more suitable for underfloor heating, as it requires a lower temperature. However the COP could fluctuate a lot with the outside temperature. In Europe, the average temperature is 10 °C and the heat pump would have a COP around 4. It means that when consuming 1kW of electrical power, the system gives 4 kW of thermal power.

The speed of the scroll compressor has the effect of decreasing the COP, as illustrated in Figure 3.13 (b). It would then be better to foster lower speed of the compressor.

3.3.5 Plate heat exchanger performance

Since most of the tests were performed in heating mode, the plate heat exchanger were be analysed to evaluate the condensing capacity of the heat pump.

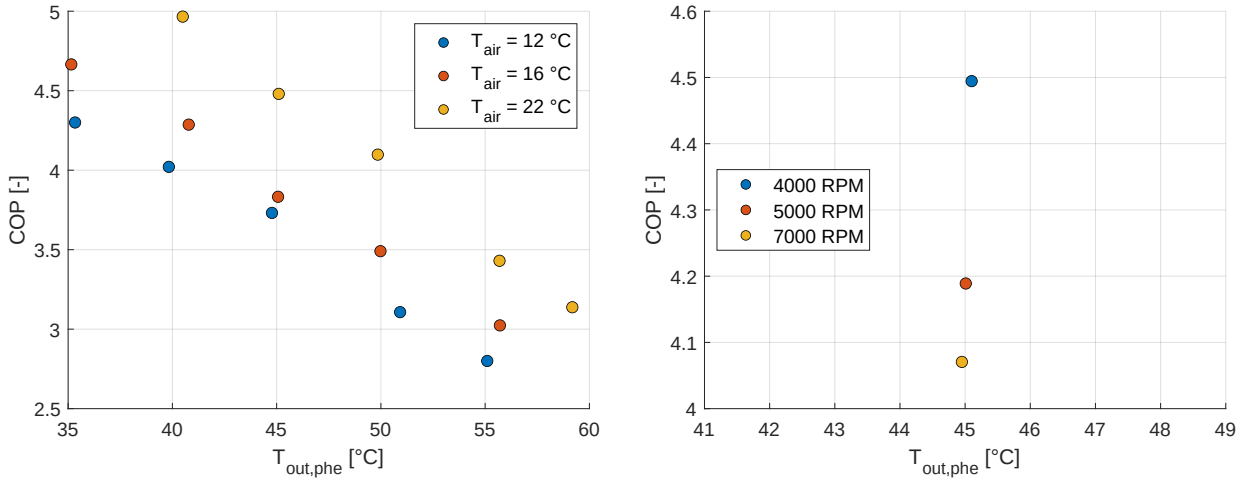

(a) (b)

Figure 3.13: Coefficient of performance of the heat pump at 5000RPM, as a function of T_{air} and $T_{out,phe}$ at 5000 RPM (a) and influence of the rotational speed (b)

The Figure 3.14 is the evolution of the useful heat described by equation (3.8) as a function of the mass flow rate of the refrigerant for all tests. $\dot{Q}_{phe}$ increases proportionally to the mass flow. Heat exchange is greater when the compressor is running faster. This could have been predicted by equation (3.5), since $\dot{m}_r$ is linearly dependent on N. The heat pump could provide 10 to 18 kW of thermal power.

Subcooling at the plate heat exchanger increases when the saturation temperature is increased, as illustrated in Figure 3.15. What matters is that it is always positive, which means that the electronic expansion valve operates with liquid phase of the refrigerant. As subcooling increases, the heat exchanger loses efficiency. In fact, when the subcooling increases, it means that there is more liquid phase in the plate heat exchanger and it has less heat capacity than the gas. It would be better to have it as low as possible, but still enough to protect the EEV, that is, at low saturation temperature.

3.3.6 Electronic expansion valve

The electronic expansion valve controls the superheat at the level of the finned exchanger, at the supply line of the compressor. The overheating fluctuates from 2 ° C to 5 ° C for the entire test matrix. The EEV adapts its opening to stay as close as possible

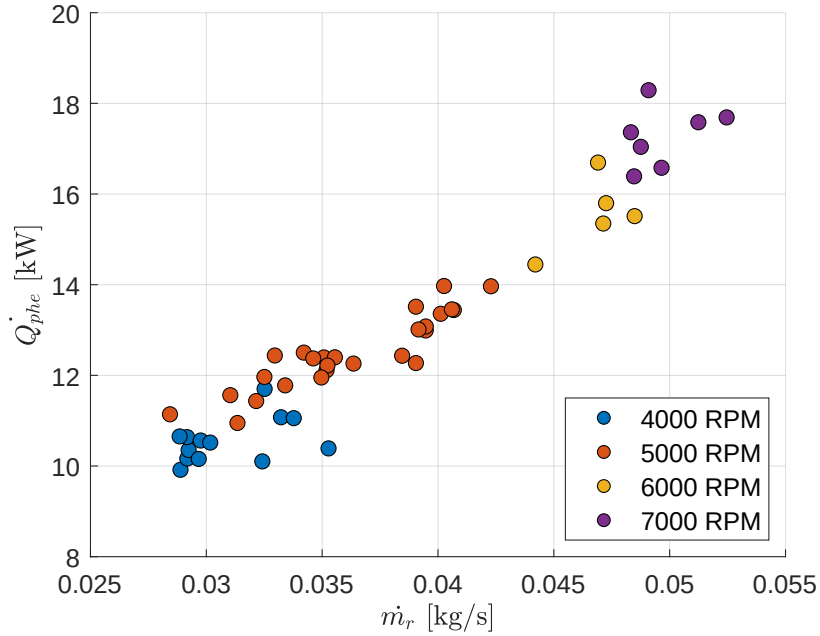

Figure 3.14: Evolution of the heat load with the refigerant mass flow rate

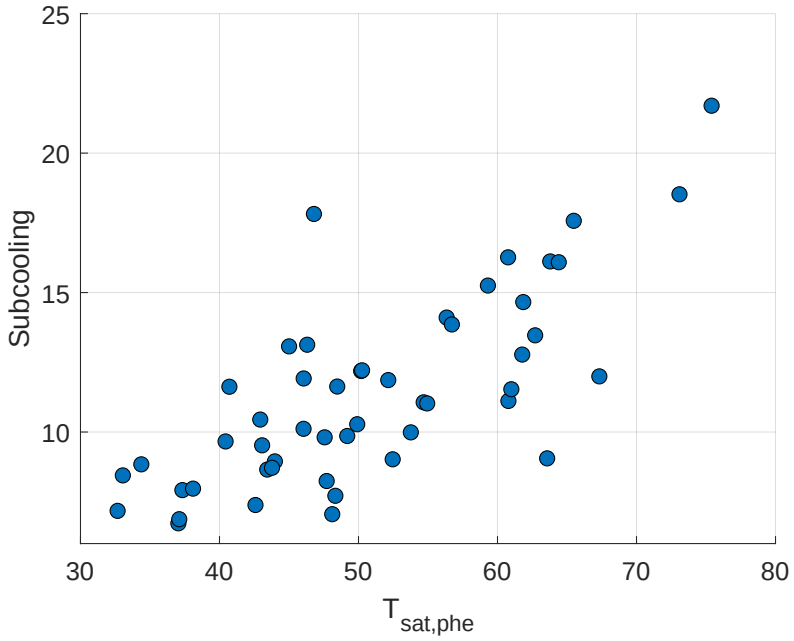

Figure 3.15: Plate heat exchanger subcooling as a function of condensing saturation temperature

to the set point, which is at 5 ° C. It is important to have a gaseous phase in the compressor, but a strong superheat would considerably increase the work of compression and decrease the COP.

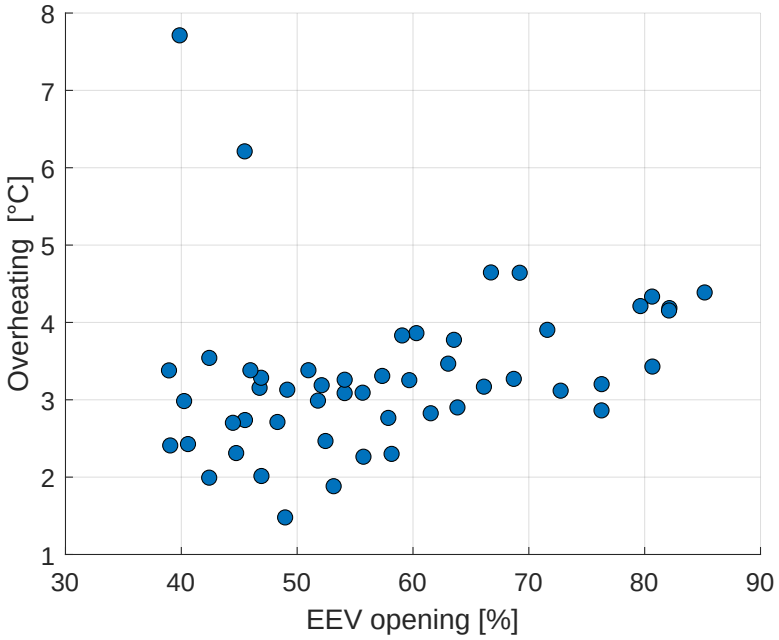

Figure 3.16: Fin heat exchanger overheating as a function of expansion valve opening

3.3.7 Safety switch

The safety switch should shut down the compressor when the pressure exceeds its maximum which is fixed at 30 bars. Figure 3.17 shows a test at 5000RPM, outside temperature of 14 °C and water temperature of 60 °C. As already said, when increasing the water temperature with the three-way valve, it increases the saturation temperature and the pressure in the plate heat exchanger. A bad reading of the pressure sensor can be spotted, as in figure 3.2. Pressure directly drops when the safety switch is actioned at 30 bars, which means that it works correctly.

3.3.8 Fans consumption

The fans blowing air on the fin heat exchanger consume approximatively 590 W to 620 W depending on the air temperature. As shown in figure 3.18, the consumption of the fans increases slightly with cold air.

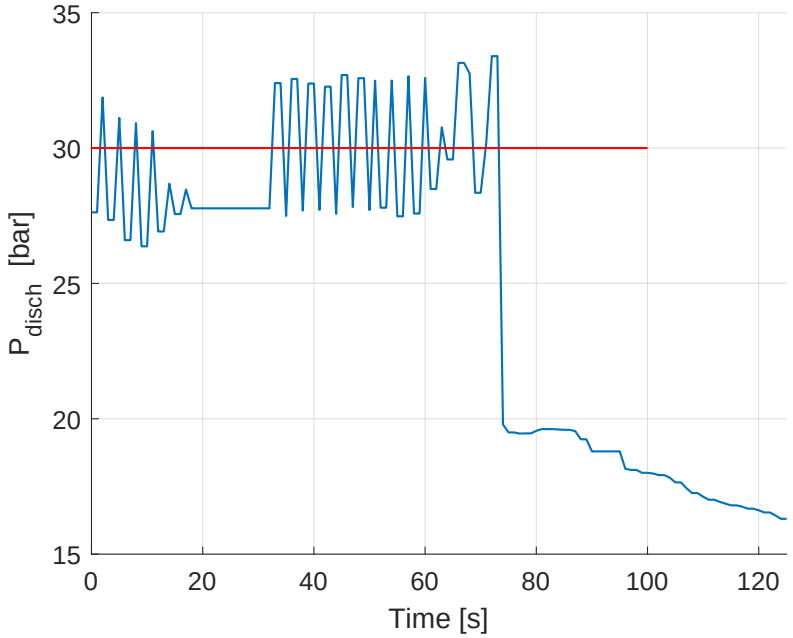

Figure 3.17: Safety switch actioned

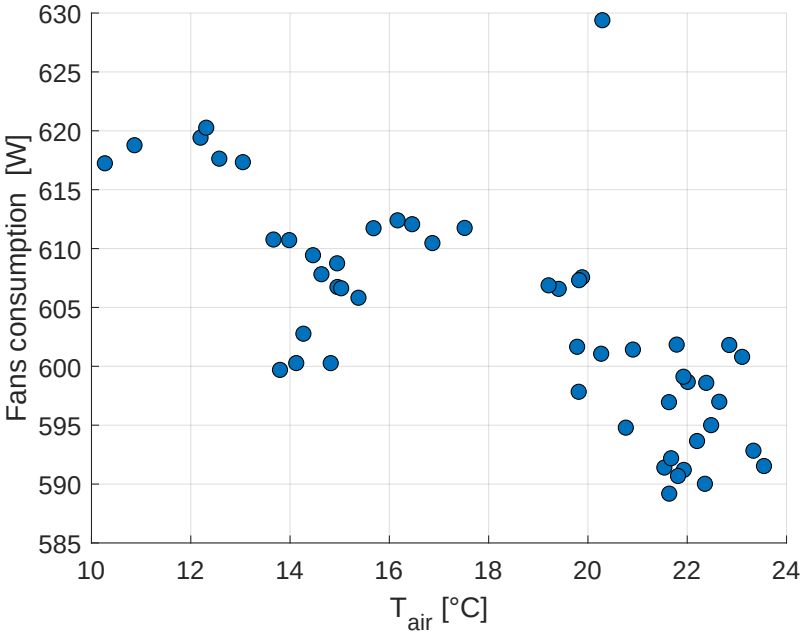

Figure 3.18: Fans consumption (a) and influence on the COP (b)

3.4 Cooling mode

The cooling mode of the heat pump has been tested by moving the four-way valve. Condensation now occurs in the finned heat exchanger, transferring heat to the air

while evaporation takes place in the plate heat exchanger, cooling the water. As a reminder, refrigerant flows now it the opposite direction in the heat exchangers. Temperature sensor T_{disch} is no more reliable since it is placed after the four way valve, not directly at the discharge line of the compressor, $T_{fhe,cp}$ should be used instead. As for the heating mode, the test was recorded in steady state for 5 minutes and the average values is studied. The test was carried out at a compressor speed of 4000 RPM, with the objective of achieving water at 7°C for cooling. The temperature of the outside air was 17.5 ° C.

The cooling test gives the temperature-entropy diagram in Figure 3.19. The blue loop represents the refrigerant cycle. The saturation level in the fin heat exchanger is 30.7 ° C, hotter than the air in the outside, while the evaporation level is -1 ° C, which approximately cools the water glycol of the user side from 10 ° C to 6 ° C (orange line).

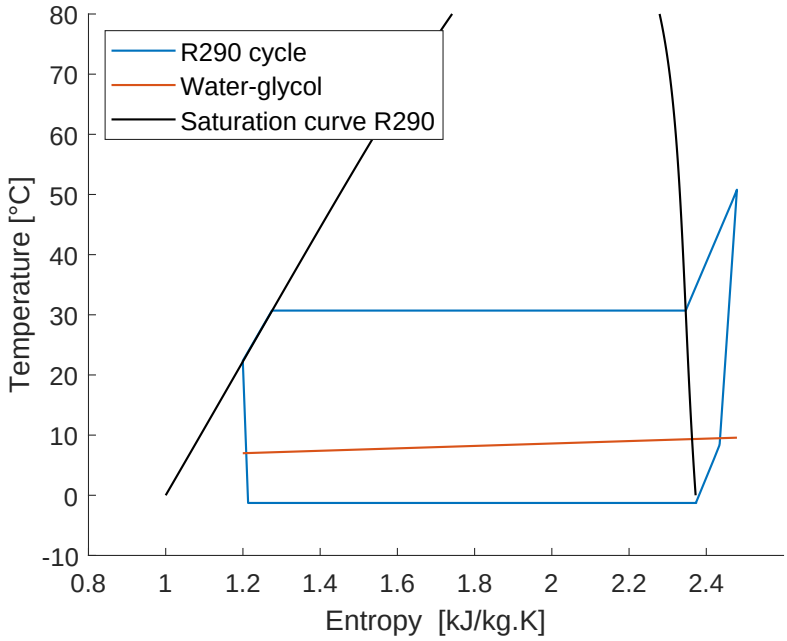

Figure 3.19: T-s diagram of the cooling mode test

The heat load is 6550 W while the compressor and the fans consume in total 1128 W + 584 W = 1712 W. Therefore, the EER (equation (3.10)) of the heat pump is 3.8.

The overheating at the plate heat exchanger is 7.2 °C in steady state, which is not

the set point. Indeed, when looking at the EEV opening in Figure 3.20 throughout the test, including the transient phase of the system, the valve is almost always fully open. This could be explained by the fact that the EEV is not really suitable for a cooling operation, and needs a bigger opening to reach the 5°C setpoint.

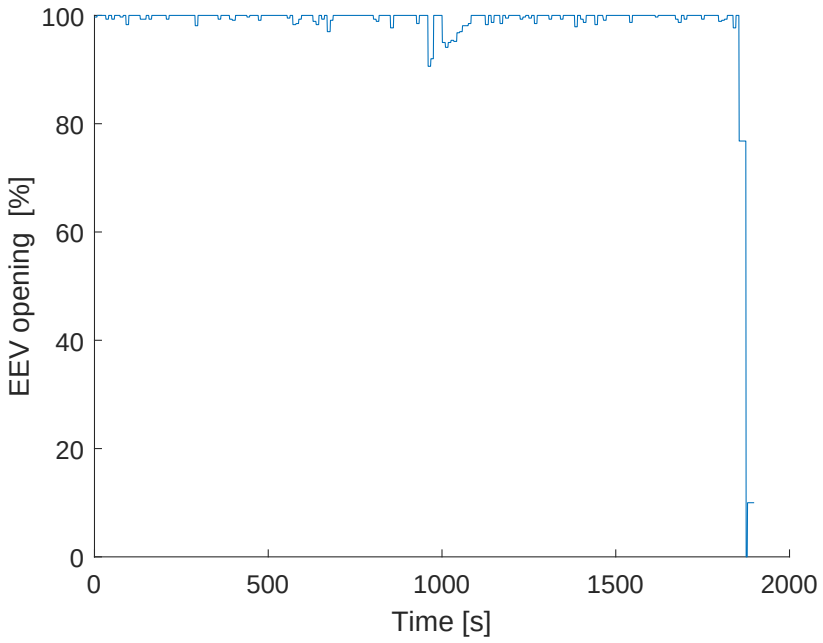

Figure 3.20: EEV opening in cooling mode

Chapter 4

Heat pump model and case study

In recent years, the building heating market has been affected by fluctuating fuel prices and even more so now with the Russian war. The choice of alternative energy sources is very important to ensure sustainable development while being competitive and respectful of the environment. *Mitis* focus their research on a natural gas turbine which is an efficient technology. The objective is to introduce the product in an off-grid complex. Indeed, the retail price of electricity is significantly higher than wholesale price, prosumers have a clear advantage at maximizing their level of self-consumption [36].

This chapter constitutes the second part of the master thesis and is focused on a study case of *Mitis*. A detailed dynamic model of the whole problem is studied with Dymola, a Modellica language program, devlopped by *Dassault Systèmes*. The program is object-oriented software, allowing to predict dynamic behavior of systems over a certain period. The model is described using open-source libraries:

-"Greenhouse" which is a library for the simulation of greenhouse climate and energy systems. It is developed by researchers from the Uliege Thermodynamics Laboratory, mainly Queralt Altes-Buch.

-"Buildings" which is a library with models for building energy and control systems [37].

-"Modelica Standard Library" which is the standard package of Dymola.

Dymola (Dynamic Modeling Laboratory) is a tool for modeling and simulating embedded and complex systems, intended for use in many applications such as automotive, aeronautics, robotics, process, etc. The graphical interface allows the user to manipulate objects and to create more complexe systems. Each object is modeled in Modellica

language, and most of them have input, output and parameter and are considered having a black box.

The system is made up of a cogeneration unit, a hot water storage tank and a condensing boiler. Every device is directed by logical regulation controller, implemented in dymola. The heat load is fully studied by Hugo Luca, another internship student at *Mitis*. The case study is an apartment building project located in Ans, near Liège. The simulations are made over one year and the economical impact is studied.

The user interface of the project in Dymola is shown in Figure 4.1. The pink box represents the logic controller, the blue the heating system and the red the user load model. Those frames are detailed in the following sections.

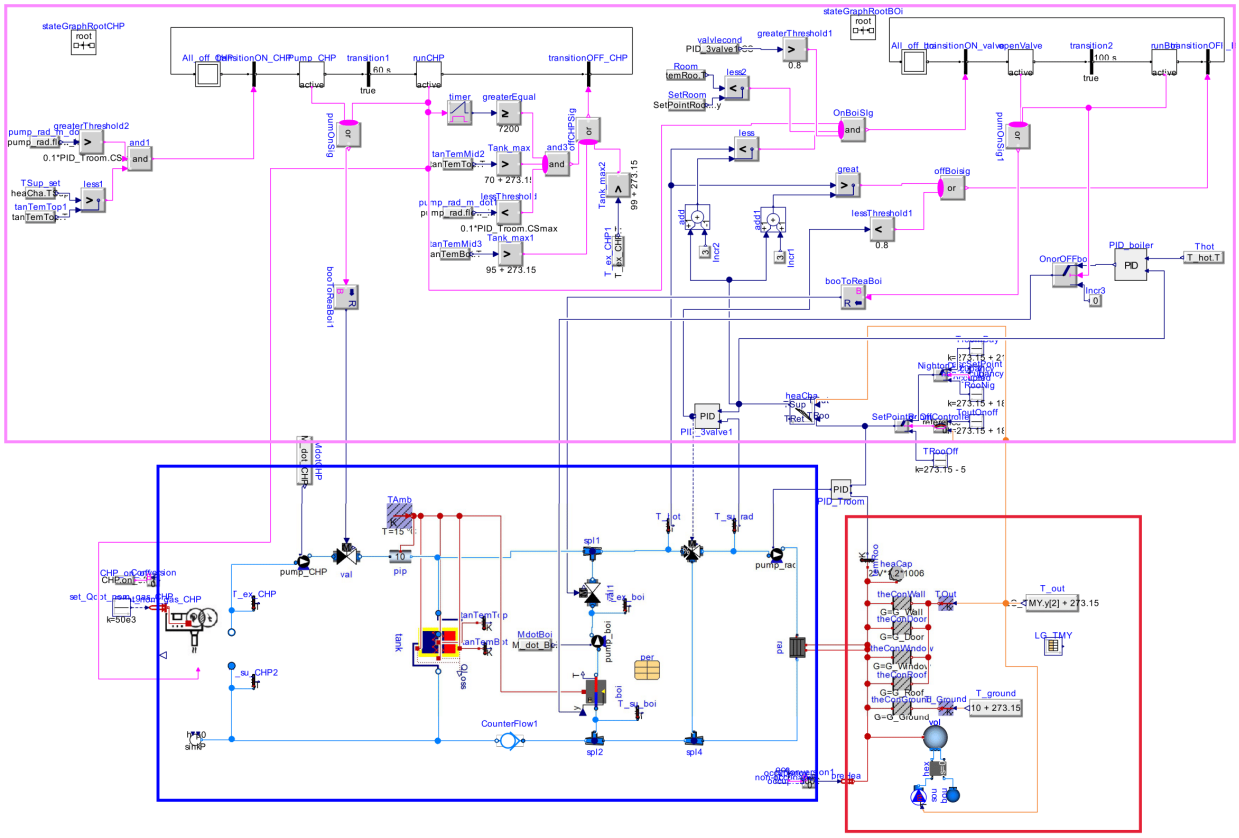

Figure 4.1: Dymola graphical interface of the project

4.1 Heating demand overview

The heat load is a 25 appartments building situated in Ans. As already mentioned, the heating demand has been studied by Hugo Lucas, the other internship student at *Mitis*. Its results gave the thermal conductance of the building envelope as well as the annual consumption (92 MWh). The objective is to match this annual consumptions with the simulation, by modeling the load with losses changing over time, to have a dynamic overview of the problem. Figure 4.2 shows all the exchange done in the room, the radiator, and the outside air. Heat is exchanged with the outside through walls, windows, doors, roof and the ground. Their thermal conductances (G) and areas are resumed in Table 4.1. A security factor of 1.1 has been multiplied, to have a certain margin regarding the results and to match the annual consumption. Floors and walls between different rooms are not taken into account because the temperature is assumed to be uniform in all apartments. Thus, only one room is modeled by a volume $V = 5712m^3$ and a thermal capacity of $\mathsf{C} = V \times 1.2 \times 1006 J/K$. The ground is assumed to be at a constant temperature of 10 °C.

The building is subject to ventilation to regulate air quality. According to the SPW wallonia energy [38], the normalized airflow for residential buildings is 3.6 m^3/h, per m^2 habitable. Since the total floor surface aera is 2284 m^2, the airflow is fixed at $3.6 \times 2284 \times 1.2 \times /3600 kg/s$. The ventilation is supposed to be double flow, which means that the outside air is preheated with the ambient air of the room.

The radiators and the people represent the source of heat. Human heat has been fixed to 100 W, which is the mean value between winter and summer according to e$^+$nergie [39]. A schedule has then been set, indicating the presence or absence of the people in the buildings. The set room temperature follows the schedule of occupancy and is set to 21 °C when occupied otherwise 18 °C.

Element	Roof	Doors	Windows	Walls	Ground
G [W/(m^2·K)]	0.12	1.15	1.5	0.12	0.2
Area [m^2]	1164	20	225	425	554

Table 4.1: Thermal conductance and area results of the buildings

The temperature of the outside air is an important parameter, since the building

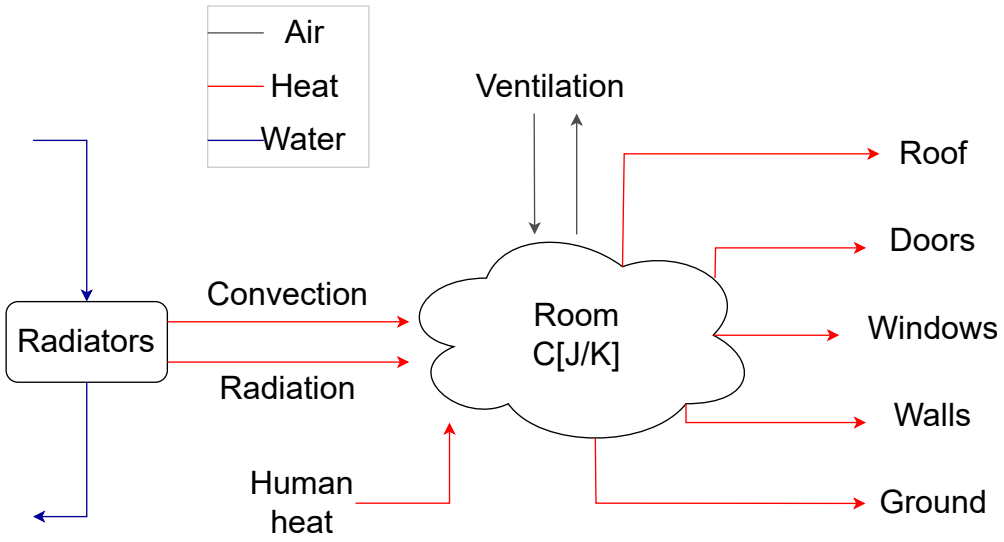

Figure 4.2: Diagram of the heat load model

exchanges through its envelope and with the ventilation. It is possible to generate a fictive annual climate thanks to the online tool TMY generator (Typical Meteorological Year) developed by the *European Commission* [40]. The fictive outside temperature is plotted in Figure 4.3, as a function of the day. With day 0 being January 1, temperature peaks can be spotted in the middle of the year in the summer and it seems to be plausible.

All of those features give the thermal load of Figure 4.4. The graph on the left is the instantaneous heat load and the graph on the right is the accumulation of heat demand. At the end of the simulation, the heat demand is 90.984 MWh which is 98 % of the calculated demand by Hugo Luca. The simulation results seems to be plausible since the load is lower in the summer (day 200). The peak consumption is in winter and is around 40kW.

4.2 Heating system

4.2.1 Overview

It is important to find a strategy to maximize the heating device production and efficiency. The main objective is to increase the running time of the CHP, since it is the main product of *Mitis* and it produces both heat and electricity.

Figure 4.5 is a schematic of the whole heating system, the blue being the path

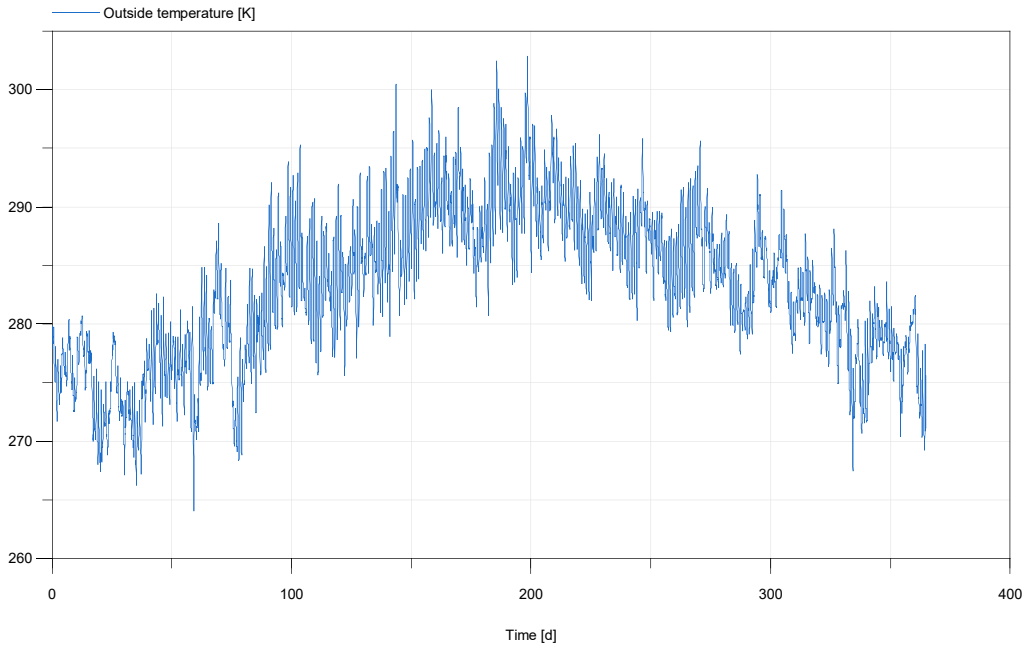

Figure 4.3: Outdoor temperature result from the European Commission's online tool TMY generator

of water. Electricity is directly consumed by the building or sold to the grid. Heat is provided to the load or stored in the water tank. The CHP is equipped with a hydraulic pump P1, feeding the stratified tank or the load directly, or both. The valve V1 is there only to ensure that there is no water coming from the CHP when it is not running. In the real case, most pumps lock when turned off, so no V1 valve is needed.

The tank is parallel to the CHP and the rest of the system, which allows to be charged or discharged when needed. A tank with an inside heat exchanger could also be a choice, but this would increase the system complexity because of the 4 ports instead of 2 like here and also the heat losses would be bigger because of the heat exchanger efficiency. Moreover the installation costs are reduced. Furthermore, the system should not be decoupled since the CHP should run most of the time, not only when the tank is cold.

The heat load is modeled by a radiator, releasing heat by radiation and convection. P2 pump represents the user pump and is activated to produce the right amount of heat in the load. The load loop is equipped with a three-way valve V2, always necessary

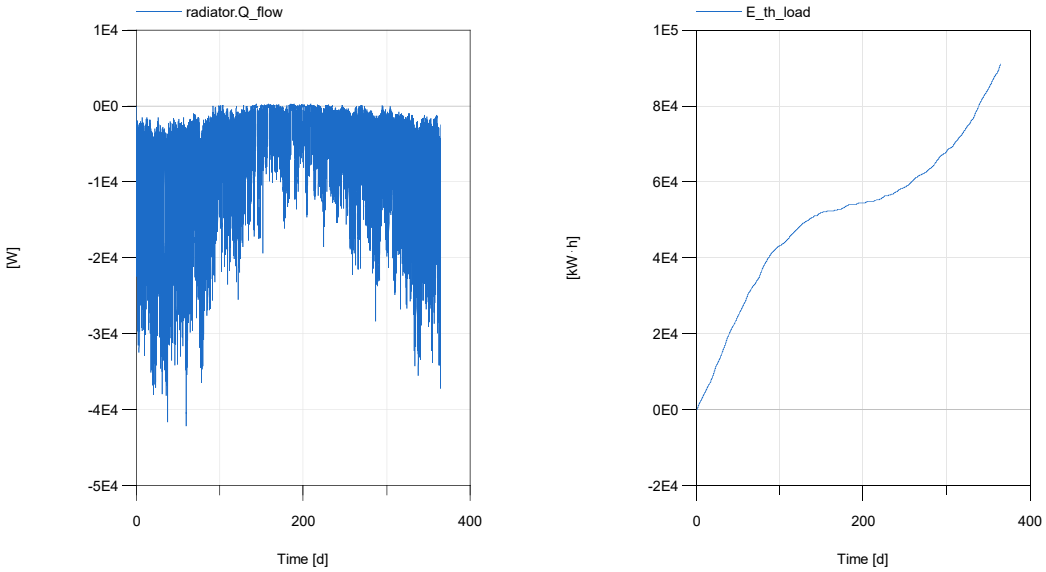

Figure 4.4: Radiator heat flow (left) and accumulation of the thermal energy over the year (right)

when a certain temperature is needed in radiators, as for the first part of the thesis. For example, the lower the room temperature, the higher the inlet temperature of the radiator must be.

Finally, a boiler is added to ensure that the heating demand is always satisfied even in winter peak periods. The pump P3 is activated when the boiler is running to be sure that there is no overheating. V3 is used that same way as V1. The reason why the boiler is in parallel is that they are both more efficient at low temperature while the CHP is more efficient at high temperature. Moreover this provides an additional mixing which stabilises the system.

Several situations of the system are then possible.

- The tank is completely filled with hot water and the charge pump P2 draws all its water from it. V1 and V2 are closed.
- Cogeneration works when the tank is no longer sufficient and provides an additional

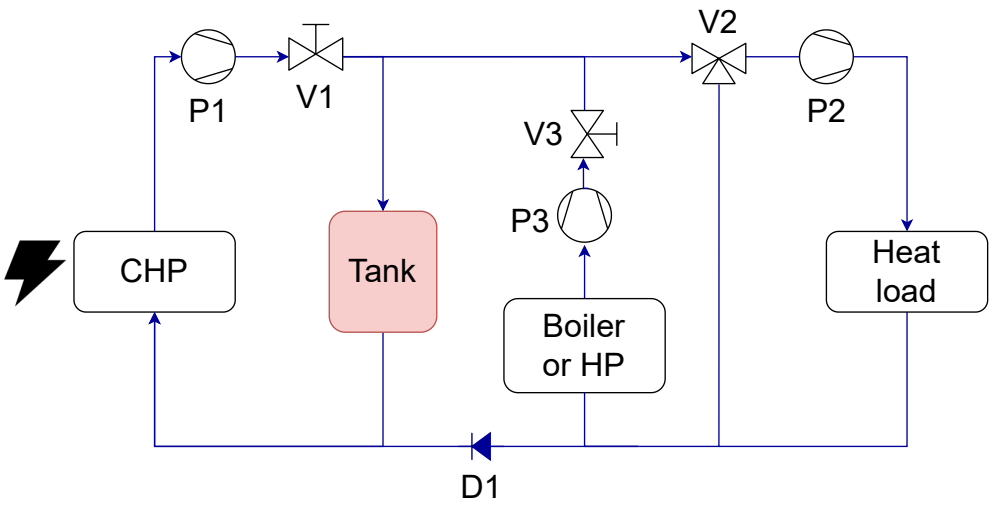

Figure 4.5: Diagram of the heating system strategy

heat source. V1 opens.

- V3 opens and boiler starts when the CHP is not enough to cover peak demand. D1 is there to prevent from drawing water from the bottom of the tank.
- The CHP is still running and the load does not need all of its heat. The tank is recharging. V3 is closed and V2 is not fully open.

Heat losses to the environment were introduced in the pipes and the tank, the heating system assumed to be in the cellar at 15°C. The logic controller manage all the device activation/deactivation and will be detailed in the section 4.3.

4.2.2 CHP unit

The combined heat and power unit is the one from the Greenhouse library. It is described as a performance-based model with constant natural gas consumption $\dot{m}_{gas}$ and constant total efficiency η_{tot}. The electrical and thermal powers are described by the following equations:

$$\dot{W} = U_{on,off}.\eta_{el}.\dot{Q}_{gas} \tag{4.1}$$

$$\dot{Q} = U_{on,off}.(\eta_{tot} - \eta_{el}).\dot{Q}_{gas} \tag{4.2}$$

where the boolean variable $U_{on,off}$ is the status of the CHP and where the electrical efficiency η_{el} is defined by the nominal second-law efficiency η_{II} and the efficiency of

Carnot η_{Carnot}:

$$\eta_{el} = \eta_{II,n}.\eta_{Carnot} \tag{4.3}$$

The micro-Ten consumes 1 g/s of natural gas which has a High Calorific Value of 49.828 MJ/kg. Thus, the CHP receives roughly 50 kW from the gas. The turbine is designed to produce 31.23 kWth and generates 11.94 kWe. The global efficiency η_{tot} is 86.9 %. The electrical and thermal efficiency has to be 23.9% and 63% respectively to match the electrical and thermal power.

When simulating over the year defined previously, Figure 4.6 is obtained. The on-off behavior is easily noticeable and the powers correctly matches the real ones. One can already notice that the turbine is less activated in the middle of the year which corresponds to the hot seasons.

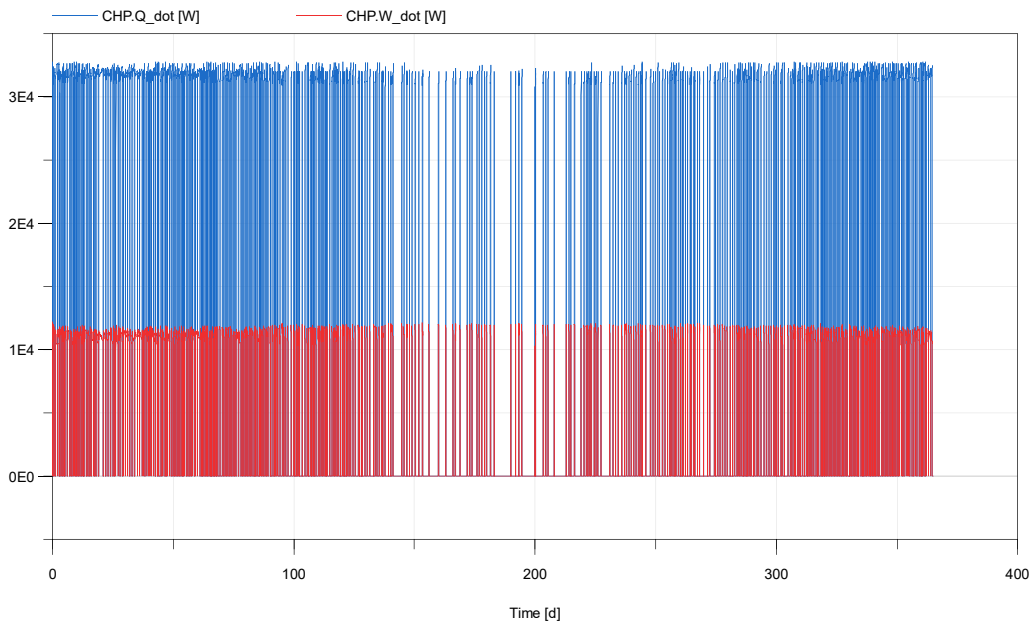

Figure 4.6: CHP electrical and thermal power over one year

4.2.3 Storage Tank

Several storage tank models are available in the libraries.

The one from Greenhouse is a stratified tank with an interval exchanger. The energy and mass conservation principles are applied and thermodynamic equilibrium is assumed at all times inside the control volume.

The building library proposes 3 different models. They are divided into segments to represent the different temperature layers as they are stratified. They differ by their inlet/oulet ports. The chosen one has one port at the top and one at the bottom. This is exactly what is needed. When the tank is charging, hot water enters at the top and only cold water exits at the bottom. When discharging, the hot water is sucked directly from above. It is also possible to introduce heat loss through an insulating membrane.

The volume of the tank is $2m^3$ and the insulation is $5cm^2$ of wood fiber which has a specific thermal conductivity of $0.038W/mK$. It is 2 m heigh and divided in 10 segments in the model.

4.2.4 Heat pump

First, a heat pump was intended to meet peak demand instead of the boiler, but the results section 4.4 will show that the boiler is a better economical choice. The model was nevertheless studied on dymola. The air to water heat pump of the Greenhouse library uses the "Consoclim" model developed by the "l'Ecole des mines de Paris". This model allows to predict the behavior of a heat pump based on three polynomial laws. The EIRFT (4.4) and CAPFT (4.5) gives respectively the COP and the heating capacity as a function of the outside temperature and the water temperature.

$$EIRFT = \frac{COP_{nom}}{COP_{fl}} = C_0 + C_1.\Delta T + C_2.\Delta T^2 \tag{4.4}$$

where $\Delta T = \frac{T_{air}}{T_w} - (\frac{T_{air}}{T_w})_n$

$$CAPFT = \frac{\dot{Q}_{fl}}{\dot{Q}_{nom}} = D_0 + D_1.(T_{air} - T_{air,nom}) + D_2.(T_w - T_{w,nom}) \tag{4.5}$$

The third law gives the performances at partial load.

$$EIRFPLR = \frac{W_{pl}}{W_{fl}} = K_1 + (K_2 - K_1).PLR + (1 - K_2).PLR \tag{4.6}$$

where $PLR = \frac{\dot{Q}_{pl}}{\dot{Q}_{fl}}$.

4.2.4.1 Calibration parameters

The experimental campaign carried out in the first part of the thesis was not large enough to completely characterize a model. Indeed the outside temperature could not be chosen, and the beaches are quite restricted. Thus, the calibration parameters have been found by manufacturer's data. Datas from *Enerblue* of a air to water propane heat pump are used. The data are available in appendix A. For instance, Figure 4.7 is the calculated EIRFT in blue dot versus the polynomial law as a function of the ΔT. The regression is done in EXEL and gives $y = 13.434x^2 - 6.286 + 1.065$. The calibration parameters are resumed in Table 4.2. No partial load is informed so the default K_1 and K_2 are chosen, moreover, the heat pump in the problem is in on/off regulation at full load.

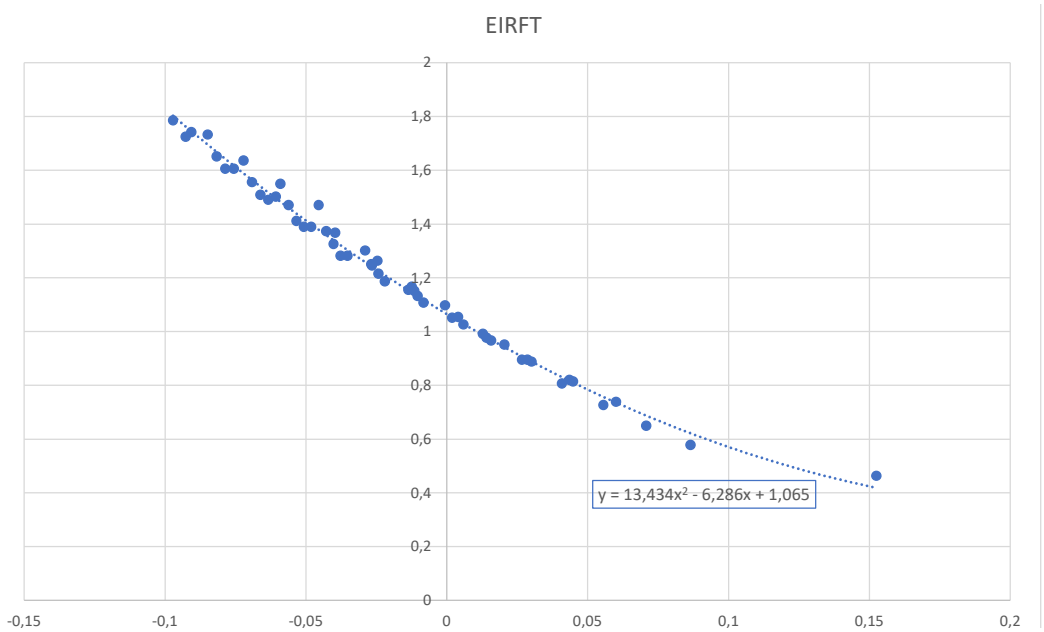

Figure 4.7: EIRFT curve

4.2.4.2 Model validation

The calibration parameters are injected in the GreenHouse heat pump model. Figure 4.8 shows the validation model of the heat pump. The power is injected, an air flow

Parameter	*Enerblue* heat pump
C_0	1,065
C_1	-6,286
C_2	13,434
D_0	0,9386
D_1	0,02132
D_2	-0.0042
K_1	0
K_2	0.67
COP_n	3.5
$\dot{Q}_n$ [kW]	29

Table 4.2: Calibration parameters

("sourceMdot" in the figure) and a water flow ("sourceMdot1" in the figure) are created, which correspond to the manufacturer's data (appendix A). Since the heat pump was designed to have a 5°C difference at the condenser, water at minus 5°C of the target temperature is injected ("sourceMdot1"). The output is the COP and is compared to the experimental one for each tests at $T_w = 30$°C, $T_w = 45$°C and $T_w = 60$°C in Figure 4.9. The model is reliable and could be used to represent a real heat pump in a system.

4.2.5 Condensing boiler

The condensing boiler is described by a performance curve in tabular form as a function of temperature. A pre-implemented map from the building library is chosen and used to match a typical oil condensing boiler. Figure 4.10 shows that the efficiency map for different fire rates. It decreases when increasing the temperature which confirms the fact that the boiler must be in parallel, at a lower temperature. It is logical, the lower the temperature, the better the condensation. It is on-off regulation and the nominal heating power is 10 kW.

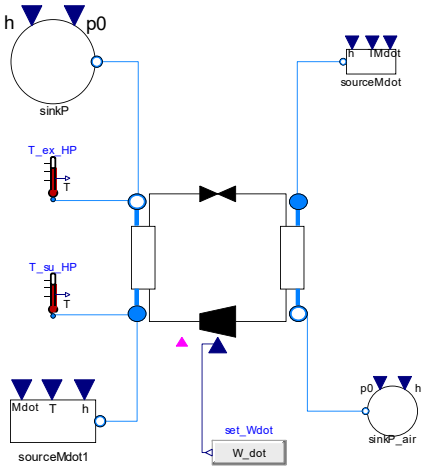

Figure 4.8: Heat pump validation model

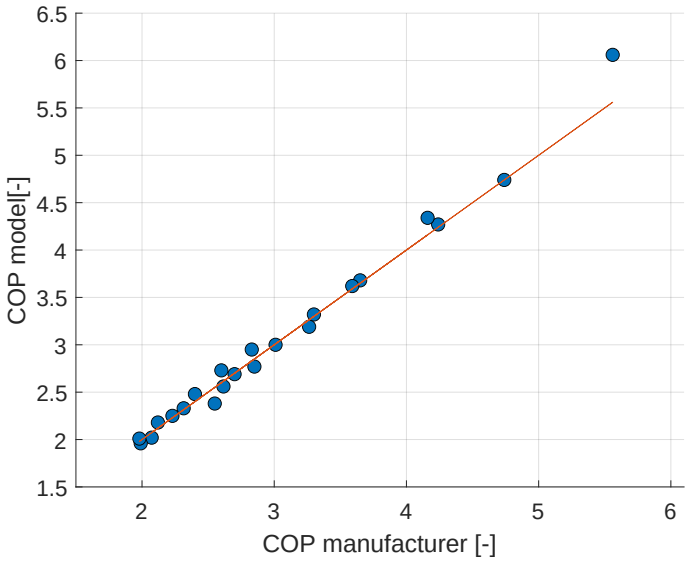

Figure 4.9: Comparison between the manufacturer's COP and the model COP at full load

4.3 Logical controller overview

The objective now is to match this heat demand with the CHP, the tank and the boiler or heat pump. This is done in Dymola by implementing a logical controller to control all the devices of Figure 4.5. The CHP is priority and the boiler or heat pump is only activated to cover peak demands.

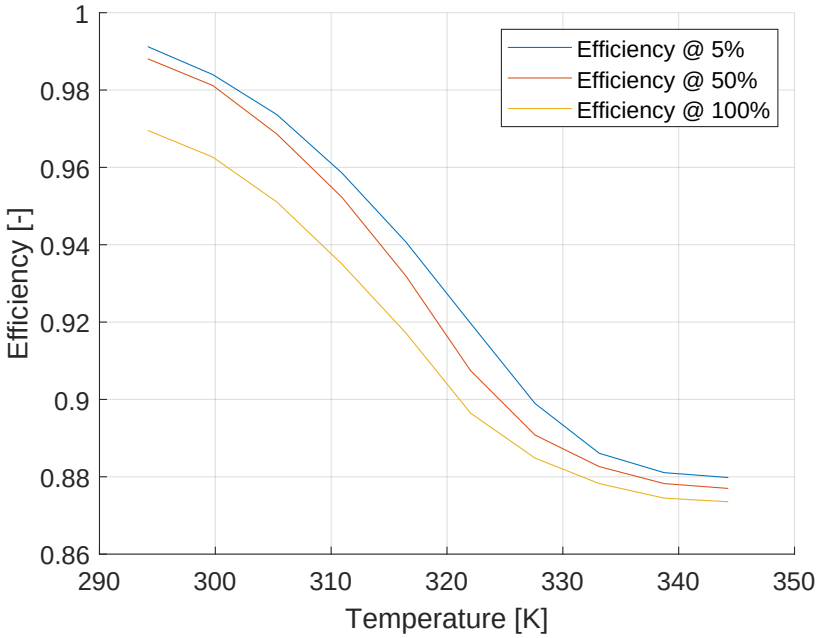

Figure 4.10: Boiler efficiency map as a function of the temperature

- The pump P1 is activated on condition that the mass flow rate at the radiator is a least 10 % of the maximum mass flow rate of P3, to avoid any error of singularity in the program. The second condition is that the top tank temperature is below the set temperature of the radiator,which means that the hot water tank is no longer sufficient. When only the CHP is activated, the mass flow rate is fixed at 3 kg/s, which is the maximum of the P3 pump. If the boiler is also required, the flow is adapted with a certain ratio $ratio_{\dot{m}}$, to respect the balance of the mixing flow. This ratio will be determined in the experimental results section. The CHP is activated only when the pump P1 is running during at least 60 seconds. The condition for stopping the turbine is that the cogeneration has been running for at least 2 hours, to avoid a too short on-off transition, and that the temperature of the reservoir is above 70°C. Indeed, the turbine must be turned on and consumes energy. The on-off cycle should be reduced. A safety feature has been added: the cogeneration switches off in an emergency when the outlet temperature is higher than 100°C.

- The pump P3 is regulated by a PID to reach the room set temperature. It varies from 0 to 3 kg/s. This maximal flow rate has been chosen to be sure that the peak

demands of 40 kW (Figure 4.4) is covered.

- The three-way valve regulates the inlet temperature of the radiator, by mixing more or less the return temperature with hot water. A tool in the building library is already implemented and gives the supply temperature setpoint of any radiator according to the outdoor temperature and the setpoint room temperature. A PID is then used to regulate the opening of the three-way valve.

- The boiler is turned on if the supply temperature of the radiator is 2°C below its set point, and if the three-way valve is fully open and if the room temperature is 2°C below its set point. In this situation, the CHP is clearly not sufficient and needs an additional heat source to cover the heat demand. The 2 °C margin is added to be sure that the fluctuation does not come from system oscillation or PID oscillation. Once again the boiler will only be able to start if the P2 pump has been running for 60 seconds beforehand. The pump water flow rate is fixed with the ratio defined at the CHP point. This heating device is turned off when the supply temperature is 2°C above its set point and when the Three-way valve is not fully opened anymore.

4.4 Results

The results of the present case are presented in this section. Table 4.3 resumes the main parameters of the heating system, the load and the market price. The selling price has been set at 47 €/MWh which was the reference rates of EDF in 2020 [41]. It was assumed that all the electricity produced is sold to the grid, since the electrical profile of the load is not known in the present case. The market price of primary energy sources varies a lot, therefore the price of natural gas is assumed to be constant throughout the year and is set at 70 €/MWh.

The influence of the ratio CHP-boiler mass flow rate $ratio_{\dot{m}}$ is first studied. Table 4.4 shows that the operating time of the CHP decreases a lot when decreasing the ratio, which means that the flow rate at the boiler increases and decreases at the turbine intercooler. In the controller, the CHP is emergency deactivated when the outlet temperature is too high. Since the mass flow rate decreases, the temperature increases faster and this could be dangerous. This has the effect of increasing the on/off cycle of the turbine, something that is not desirable in the system, since it is set to run

Description	Variable	Value
CHP thermal capacity	$\dot{Q}[kWth]$	31.23
CHP electrical capacity	$\dot{W}[kWe]$	11.94
Thermal energy storge	V $[m^3]$	2
Boiler capacity	$\dot{W}_{boi}[kWth]$	15
CHP total efficiency	η_{tot}	0.86
HP nominal COP	COP	3.5
Annual thermal load demand [MWh]	$\dot{E}_{th,load}$	90.8
Selling price of electricity	$\pi_{el,sell}$ [€/MWh]	50
Price of natural gaz	π_{gas} [€/MWh]	70
Price of heating oil	π_{HO} [€/MWh]	10

Table 4.3: Main parameters of the models

at least 2 hours. Thus, a higher ratio is preferable: it is set to 0.5 because in terms of operating time, it does not change a lot to increase it more. moreover, it ensures that the temperature at the boiler does not increase too much to avoid efficiency drop (Figure 4.10).

Ratio mass flow rate CHP-boiler	0.1	0.3	0.5	0.7	0.9
CHP operating time	2675	2861	2993	3011	3017
Boiler operating time	1448	762	273	200	187

Table 4.4: Influence of the ratio CHP/boiler mass flow rate

It would be very oversized to place a heat pump instead of the boiler. Indeed the boiler is running only 273 hours which is only 3% of the year.

As shown in Table 4.5, the total heat generation is 97.29 MWh/y which is 7% bigger than the demand. The difference comes from the heat losses introduced at the tank and pipes. Since all the electricity is sold to the grid, 1578 could be saved on the gas invoice. If all the electricity is directly consumed, the savings would be around 5000 € if it is assumed that the electricity price is 150 €/MWh.

Figure 4.11 is the running time accumulation of the boiler and the CHP over the

year. The turbine is running roughly 3000 hours while the boiler only 275. This really means that CHP has priority in the controller and the boiler is only used to cover peak demand. As already mentioned, this is because running the CHP requires more effort than the boiler, so the CHP has to run longer while the boiler can be switched on/off more easily. As in figure 4.4 (b), it can be seen in Figure 4.11 that the heating system is less stressed in summer, while the operating time is higher in winter.

Description	Variable	With boiler
CHP thermal generation	$\dot{E}_{th,CHP}[MWh/y]$	94.85
CHP electrical generation	$\dot{E}_{el,CHP}[MWh/y]$	33.44
Additional thermal generation	$\dot{E}_{th,sup}[MWh/y]$	2.44
Total heat generation	$\dot{E}_{tot}[MWh/y]$	97.29
Thermal load	$\dot{E}_{th,load}[MWh/y]$	90.98
Cost of gas	C_{gas} [€/y]	10440
Cost of heating oil	C_{HO} [€/y]	25
Cost of sold electcity	C_{sell} [€/y]	- 1578

Table 4.5: Main results of the models

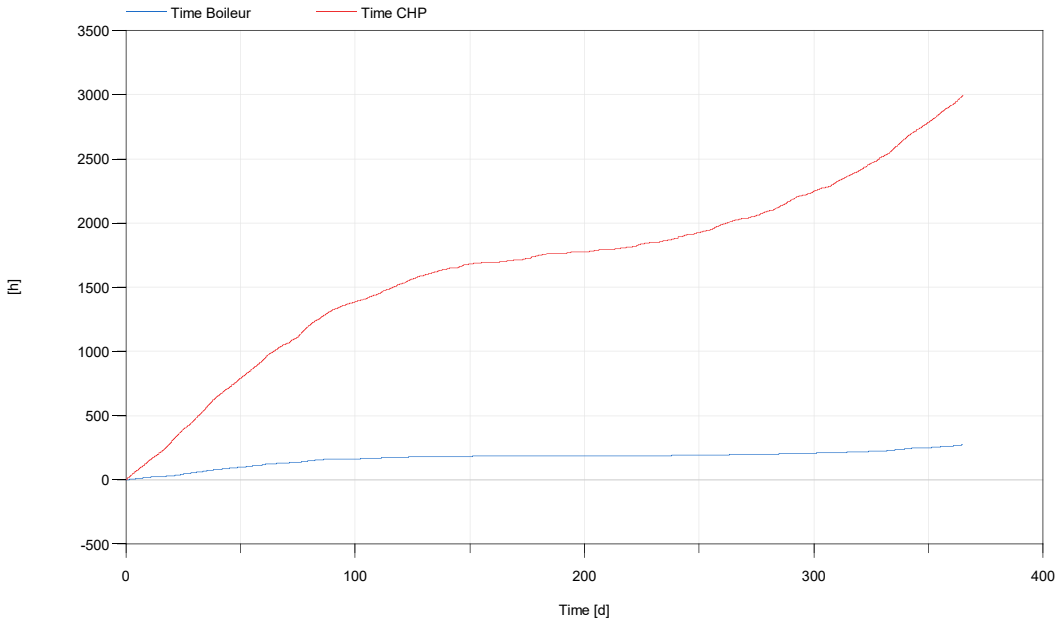

Figure 4.11: Evolution in time of the accumulated running time of the turbine and the boiler

Chapter 5

Improvements

The experimental characterization was subject to some uncertainties and faulty sensors. The Dymola model was also not entirely complete and some assumptions were made. The other perspectives below could improve the calculation part and the characterization of the heat pump.

The validation section 3.3.1 shows that some sensors were not really reliable. The evolution of the high pressure sensor was obviously not constant over time and was subject to strong oscillations. Some other temperature sensors were not good as well. Reviewing them would be an excellent idea, to have a more precise characterization of the heat pump.

The three-way valve of the user side was always driven manually. For instance in Figure 3.13, the temperature points are not really on the same vertical line, which means that they are not at the exact same temperature. The implementation of a PID controller in the Labview interface to control the hot water temperature would increase the reliability of the tests and the influence of this parameter on the heat pump performances could be better studied.

Another big issue was the outside temperature. First it was impossible to change it, and more, to keep it constant. Thus, some tests started at a certain temperature and since the outside temperature changed, the system could not be 100 % steady state. A solution to counter this could be to include the test rig in a climate chamber, where the air temperature could be controlled. Thereby, the range of air temperature could considerably increase, which is really important. The experimental campaign took place from March to June so the heat pump was only tested from 10 to 20°C whereas the temperature in most European countries can vary from -20°C to 40°C. Moreover, the

dymola model (second part of the thesis) could be adjusted and studied in real cases.

The cooling mode of the heat pump was tested once at 17.5°C. Studying it at higher temperatures would be more practical, because no air conditioning is really needed below 25°C for residential applications. It is also important to see the influence of the air and cold water temperature in cooling mode.

Figure 3.20 showed that the EEV was almost all the time 100% opened, which proves that the expansion valve is too small for cooling application. A device with a wider opening range has to be installed to allow better control of superheat at the condenser in cooling mode.

The total mass of propane has been set at 1 kg, a value found during tests carried out on previous versions of the heat pump. Maybe this is not the optimal mass of refrigerant. The influence of this parameter should also be studied.

There was no refrigerant mass flow. It was estimated by calculating it from the water-glycol mass flow rate, the temperature difference at the level of the plate heat exchanger, the refrigerant states and assuming that the heat exchanger is adiabatic. The mass flow rate of propane is however one of the most important parameters when studying the compressor, because its volumetric and isentropic efficiency are derived from it. A suggestion is to add a magnetic flow meter, which will not disturb the flow, or to implement a black box model to estimate it.

Regarding the Dymola model, the case study could also include the sanitary water and electricity demand of the buildings to complete the economic results found.

Chapter 6

Conclusion

The current climatic and political context encourages the heat pump industry to search for new technologies. Only refrigerants with very low GWP and 0-ODP are authorized in refrigerant systems. Propane is a natural refrigerant and is more and more studied in many applications including in heating and cooling systems for buildings.

This thesis focused on the experimental characterization of an air-water propane heat pump. The objective being to study its perfomances depending on the air temperature, the water temperature and the compressor rotational speed. A test bench has been set up and equipped with a series of sensors at strategic points. The user side was modeled by a water-glycol loop with fans that release heat and a three-way valve to control the temperature. The heat pump is equipped with a four-way valve which allows the cycle to be reversed and to produce either cold or heat. The actuators of the test bench were controlled in Labview, through a microcontroller and VISA communication. The circuit was filled with 1 kg of propane.

While testing the heating mode, the outdoor temperature range of the tests ranged from 10 to 22°C and the water-glycol temperature varied from 35 to 60 °C. The refrigerant mass flow rate was estimated with the assumption that the plate heat exchanger was adiabatic. It varied from 0.03 kg/s to 0.05 kg/s, increasing with the speed of rotation of the compressor. It has been noticed that the COP decreases when the water temperature and the rotational speed increase and increases with the outside temperature. Thus, the heat pump must be used for underfloor heating with a low compressor rotation speed, in order to maximize performance and achieve a COP of around 4.5.

Concerning the compressor, its isentropic efficiency is maximal at lower outside temperatures and rotational speed, with low pressure ratio and with low mass flow rate. Its volumetric efficiency is better as well with lower pressure ratio and increases when the mass flow rate is reduced. It is therefore necessary to promote operation at low rotational speed, unless a lot of heat is needed. Indeed the heat load increases with the rotational speed. The subcooling at the plate heat exchanger was bigger when the saturation temperature was high. Superheat at the compressor suction line was almost constant at 4°C for all tests.

The heat pump was also tested to produce cold but the electronic expansion valve was too small to ensure good control of superheat. The EER was 3.8 for an outside air temperature of 17.5°C and a water temperature of 7°C.

The case study was modeled and simulated during a year. The heating demand was known and the objective was to cover it with a heating strategy composed of a cogeneration device, a condensing boiler and a tank. The results show that the CHP and the boiler produces a total heat of 97.29 MWh and that the gas bill is 10440 €. The CHP runs 2993 hours while the boiler only 273 hours.

Some perspectives and possible improvements are also presented.

Appendix A

Manufacturer's data

T_air	T_w	M_dot_air [m^3/h]	M_dot_w [m^3/h]	W_cp [kW]	Q_dot_cd [kW]	COP
-20	30	17959	2.229	5,41	12,9	2,38
-15	30	17972	2.647	5,73	15,4	2,69
-10	30	17971	3.098	6	18	3
-5	30	17971	3.564	6,24	20,7	3,32
0	30	18060	4.121	6,49	23,9	3,68
7	30	18042	4.982	6,77	28,9	4,27
12	30	18026	5.677	6,96	33	4,74
20	30	6929	6.623	6,35	38,5	6,06
40	30	2633	8.095	6,24	47,1	7,55
-20	35	17959	2.618	5,57	12,6	2,26
-15	35	17972	2.618	5,96	15,2	2,55
-10	35	17971	3.031	6,27	17,6	2,81
-5	35	17971	3.505	6,57	20,3	3,09
0	35	18055	4.046	6,87	23,4	3,41
7	35	18036	4.893	7,26	28,4	3,91
12	35	18019	5.579	7,51	32,3	4,3
20	35	6532	6.476	6,98	37,6	5,39
-20	40	17959	2.107	5,71	12,2	2,14
-15	40	17972	2.524	6,13	14,6	2,38
-10	40	17971	2.968	6,52	17,2	2,64
-5	40	17971	3.433	6,87	19,8	2,88
0	40	18050	3.965	7,25	22,9	3,16
7	40	18029	4.794	7,73	27,7	3,58
12	40	17545	5.461	8,03	31,6	3,94
20	40	6132	6.323	7,59	36,6	4,82
-20	45	17959	2.031	5,8	11,7	2,02
-15	45	17972	2.445	6,28	14,1	2,25

Figure A.1: Manufacturer's data

T_air	T_w	M_dot_air [m^3/h]	M_dot_w [m^3/h]	W_cp [kW]	Q_dot_cd [kW]	COP
-15	45	17972	2.445	6,28	14,1	2,3
-10	45	17971	2.888	6,74	16,7	2,5
-5	45	17971	3.435	7,24	19,8	2,7
0	45	18046	3.877	7,6	22,4	3
12	45	16844	5.345	8,53	30,9	3,6
20	45	5716	6.166	8,2	35,6	4,3
-20	50	17959	3.314	5,87	11,5	2
-15	50	17972	2.363	6,43	13,6	2,1
-10	50	17971	2.808	6,67	16,2	2,3
-5	50	17971	3.262	7,46	18,8	2,5
0	50	18037	3.780	7,98	21,8	2,7
7	50	18020	4.572	8,68	26,3	3
12	50	16141	5.219	9,05	30,1	3,3
20	50	5292	6.001	8,84	34,6	3,9
-15	54,5	17972	1.637	6,51	13,2	2
-10	55	17971	2.726	7,3	15,7	2,2
-5	55	17971	3.164	7,76	18,2	2,4
0	55	18030	3.675	8,36	21,1	2,5
7	55	18008	4.461	9,19	25,7	2,8
12	55	15681	5.068	9,6	29,2	3
20	55	4830	5.825	9,5	33,5	3,5
-10	60	17971	2.600	7,41	14,9	2
-5	60	17971	3.066	8,09	17,6	2,2
0	60	18024	3.567	8,78	20,5	2,3
7	60	17999	4.339	9,73	24,9	2,6
12	60	14882	4.935	10,2	28,3	2,8
20	60	4374	5.651	10,2	32,5	3,2

Figure A.2: Manufacturer's data

Bibliography

[1] Wikipedia. *Politics of climate change*. URL: https://en.wikipedia.org/wiki/Politics_of_climate_change. (accessed : 02-05-2022).

[2] J. Lastennet. *La lutte contre le changement climatique en 12 dates*. URL: https://www.touteleurope.eu/environnement/la-lutte-contre-le-changement-climatique-en-12-dates/. (accessed : 02-05-2022).

[3] SPF enconomie. "Energy Key Data, février 2020". In: (2022). DOI: https://economie.fgov.be/fr/file/2970574/download?token=gpe10r7K. (accessed : 02-05-2022).

[4] Intergovernmental Panel on Climate Change. "Anthropogenic and Natural Radiative Forcing". In: *Climate Change 2013 - the Physical Science Basis* (July 2020), pp. 659–740. ISSN: 9781107415324. DOI: 10.1017/cbo9781107415324.018. (accessed : 07-06-2022).

[5] Energy +. *Réglementation des fluides frigorigènes*. URL: https://energieplus-lesite.be/reglementations/climatisation-et-refrigeration3/reglementation-des-fluides-frigorigenes/. (accessed : 07-06-2022).

[6] "Class | Ozone-depleting Substances". In: *Science - Ozone Layer Protection* (2007). URL: https://web.archive.org/web/20101210101528/http://www.epa.gov/ozone/science/ods/classone.html. (accessed : 08-06-2022).

[7] Adrián Mota-Babiloni et al. *Analysis based on EU Regulation No 517/2014 of new HFC/HFO mixtures as alternatives of high GWP refrigerants in refrigeration and HVAC systems*. 2015. DOI: 10.1016/j.ijrefrig.2014.12.021. (accessed : 08-06-2022).

[8] EPA. *Significant New Alternatives Policy (SNAP)*. URL: https://www.epa.gov/snap/refrigerant-safety. (accessed : 08-06-2022).

[9] Smarter House. *Heating Systems*. URL: https://smarterhouse.org/home-systems-energy/heating-systems. (accessed : 09-05-2022).

[10] Vissemann. *Ready for the future: The Viessmann business areas*. URL: https://www.viessmann.family/en/what-we-offer. (accessed : 08-06-2022).

[11] Sarah Molegraaf. *Boiler vs. Furnace: Which One Makes More Sense?* URL: http://celebritybuildersllc.com/blog/2017/3/2/boiler-vs-furnace-which-one-makes-more-sense. (accessed : 10-05-2022).

[12] Di Wu et al. "The performance comparison of high temperature heat pump among R718 and other refrigerants". In: *Renewable Energy* 154 (July 2020), pp. 715–722. ISSN: 18790682. DOI: 10.1016/j.renene.2020.03.034. (accessed : 11-05-2022).

[13] Batirama. *Utiliser l'eau comme fluide réfrigérant, pourquoi pas ?* URL: https://www.batirama.com/article/10226-utiliser-l-eau-comme-fluide-refrigerant-pourquoi-pas.html. (accessed : 11-05-2022).

[14] HVAC Intelligence. *Liste des fluides frigorigènes naturels*. URL: https://www.hvac-intelligence.fr/fluide-frigorigene-naturel/. (accessed : 11-05-2022).

[15] Paul Byrne, Redouane Ghoubali, and Jacques Miriel. "Scroll compressor modelling for heat pumps using hydrocarbons as refrigerants". In: *International Journal of Refrigeration* 41 (2014), pp. 1–13. ISSN: 01407007. DOI: 10.1016/j.ijrefrig.2013.06.003. (accessed : 11-05-2022).

[16] "Performance evaluation of propane heat pump system for electric vehicle in cold climate". In: *International Journal of Refrigeration* 95 (Nov. 2018), pp. 51–60. ISSN: 01407007. DOI: 10.1016/j.ijrefrig.2018.08.020.

[17] Yue Huang, Xiuchun Wu, and Jiahao Jing. "Research on the electric vehicle heat pump air conditioning system based on R290 refrigerant". In: *Energy Reports* 8 (Oct. 2022), pp. 447–455. ISSN: 23524847. DOI: 10.1016/j.egyr.2022.05.112. URL: https://linkinghub.elsevier.com/retrieve/pii/S2352484722009210. (accessed : 13-06-2022).

[18] Álvaro Roberto Gardenghi et al. "A detailed study of the transient behavior of dual-skin chest-freezer with R290". In: *International Journal of Refrigeration* 131 (Nov. 2021), pp. 300–311. ISSN: 01407007. DOI: 10.1016/j.ijrefrig.2021.07.014. (accessed : 13-06-2022).

[19] Tecumseh. *Propane R290 fluide frigorigène naturel*. URL: https://www.tecumseh.com/globalassets/media/europe/files/brochures_marketing/plaquette_r290_fr.pdf. (accessed : 11-05-2022).

[20] Energie+. *Comparer les performances des fluides frigorigènes*. URL: https://energieplus-lesite.be/evaluer/climatisation5/comparer-les-performances-des-fluides-frigorigenes/. (accessed : 11-05-2022).

[21] Enyuan Gao et al. *A review of application status and replacement progress of refrigerants in the Chinese cold chain industry*. Aug. 2021. DOI: 10.1016/j.ijrefrig.2021.03.025. (accessed : 13-06-2022).

[22] US EPA. *TRANSITIONING TO LOW-GWP - ALTERNATIVES IN DOMESTIC REFRIGERATION (pdf)*. URL: https://www.epa.gov/sites/default/files/2016-12/documents/transitioning_to_low-gwp_alternatives_in_domestic_refrigeration.pdf. (accessed : 09-06-2022).

[23] *Applications of refrigerant R1234yf in heating, air conditioning and refrigeration systems: A decade of researches*. Oct. 2020. DOI: 10.1016/j.ijrefrig.2020.06.014.

[24] Vipin Nair. *HFO refrigerants: A review of present status and future prospects*. Feb. 2021. DOI: 10.1016/j.ijrefrig.2020.10.039. (accessed : 13-06-2022).

[25] ASHRAE. *Designation and Safety Classification of Refrigerants: Addendum f to ANSI/ASHRAE Standard 34-2019(pdf)*. (accessed : 13-06-2022).

[26] Wikipedia. *Micro combined heat and power*. URL: https://en.wikipedia.org/wiki/Micro_combined_heat_and_power#Overview. (accessed : 11-05-2022).

[27] Paul Breeze. *Gas Turbine Combined Heat and Power Systems*. 2018. DOI: 10.1016/b978-0-12-812908-1.00006-7. (accessed : 11-05-2022).

[28] Paul Breeze. *Piston Engine Combined Heat and Power Systems*. 2018. DOI: 10.1016/b978-0-12-812908-1.00004-3. (accessed : 11-05-2022).

[29] Wikipedia. *Cogeneration*. URL: https://en.wikipedia.org/wiki/Cogeneration#Types_of_plants. (accessed : 11-05-2022).

[30] Paul Breeze. *Steam Turbine Combined Heat and Power Systems*. 2018. DOI: 10.1016/b978-0-12-812908-1.00005-5. (accessed : 11-05-2022).

[31] Paul Breeze. *Nuclear Combined Heat and Power*. 2018. DOI: 10.1016/b978-0-12-812908-1.00008-0. (accessed : 11-05-2022).

[32] Paul Breeze. *Fuel Cell Combined Heat and Power*. 2018. DOI: 10.1016/b978-0-12-812908-1.00007-9. (accessed : 11-05-2022).

[33] Paul Breeze. *Renewable Energy Combined Heat and Power*. 2018. DOI: 10.1016/b978-0-12-812908-1.00009-2. (accessed : 11-05-2022).

[34] Dansfoss. *Components for heat pumps – part 5: four-way reversing valves*. URL: https://www.danfoss.com/en/service-and-support/case-stories/dcs/components-for-heat-pumps-part-5-four-way-reversing-valves/. (accessed : 15-06-2022).

[35] Auteur : Müllender S. *Experimental analysis and modelling of a heat pump for a micro-CHP (Combined Heat and Power) cycle[BR]*. URL: http://hdl.handle.net/2268.2/11601. (accessed : 03-08-2022).

[36] Sylvain Quoilin et al. "Quantifying self-consumption linked to solar home battery systems: Statistical analysis and economic assessment". In: *Applied Energy* 182 (Nov. 2016), pp. 58–67. ISSN: 03062619. DOI: 10.1016/j.apenergy.2016.08.077.

[37] Michael Wetter et al. "Modelica Buildings library". In: *Journal of Building Performance Simulation* 7.4 (2014), pp. 253–270. DOI: 10.1080/19401493.2013.765506. URL: https://doi.org/10.1080/19401493.2013.765506.

[38] SPW. *Débits de ventilation*. URL: https://energie.wallonie.be/fr/09-06-debits-de-ventilation.html?IDC_PEB=9491&IDD=113691&IDC=9096. (accessed : 11-08-2022).

[39] E$^+$nergy. *Charges thermiques internes pour les bureaux*. URL: https://energieplus-lesite.be/theories/bilan-thermique44/charges-thermiques-internes-pour-les-bureaux/. (accessed : 11-08-2022).

[40] European Comission. *TMY generator*. URL: https://joint-research-centre.ec.europa.eu/pvgis-photovoltaic-geographical-information-system/pvgis-tools/tmy-generator_en. (accessed : 11-08-2022).

[41] Slectra. *Tarif rachat EDF 2022 : photovoltaique, éolien, biométhane...* URL: https://selectra.info/energie/guides/environnement/rachat-electricite-gaz-edf. (accessed : 16-08-2022).